Doctoral Dissertation
(Shinshu University)
Study on electrospun silicone modified polyurethane nanofibers

September, 2019

YIN CHUAN

Interdisciplinary Graduate School of Science and Technology

Shinshu University

Department of Bioscience and Textile Technology

Table of Contents

Chapter 1

Introduction

1 Introduction

1.1 Background

Electrospinning is a fabrication process of nanofibers through the electrically charged jet of polymer solution or melt. Electrospinning has gained much attention in the last decade not only due to its versatility in spinning a wide variety of polymeric fibers but also due to its consistency in producing fibers in the submicron range. These fibers, with smaller pores and higher surface area than regular fibers, have enormous applications in nanocatalysis, tissue scaffolds, protective clothing, filtration, and optical electronics.[1] Electrospun nanofibers form a unique class of materials to be used for biomedical application. The submicron size and high surface area along with the porous architecture of nanofibers and the nanofiber mesh closely relates them to biostructures.[2] Additionally, the flexibility of the technique to generate customized structures, with desirable surface and bulk properties, by utilizing blends and hybrids of different polymers and varying processing parameters and methods, has sparked interest in the electrospun polymers for biomedical application. In tissue engineering, electrospun mats provide support for cell attachment and growth along with the exchange of nutrients and gases[3]. The broad application of electrospun nanofibers in the field of biomedical, apart from the drug delivery include tissue engineering[4], wound dressing[5], enzyme immobilization[6], health care[7], and biotechnology. Extensive research in tissue engineering application targets the bone[8], tendon and ligament[9], vascular[10], neural[11], and skin tissue[12]. Reports indicate two-thirds of electrospinning applications are in the biomedical field[13].

Polyurethane (PU) is formed by reaction of polyisocyanates with hydroxyl-containing

compounds. (Fig. 1) Desired properties can be tailored by selecting the type of isocyanate and polyols, or combination of isocyanates and polyols.[14] Strong intermolecular bonds make polyurethanes useful for diverse applications in adhesives and coatings, also in elastomers, foams, and medical applications because of their good flexibility. Polyurethane fine nanofibers produced by electrospinning have a large surface area and porous network structure. Therefore, electrospun polyurethane nanofibers can be used effectively for many purposes in daily life: furniture, shoes, building, acoustic and thermal insulation, automobile, electronics, textile, and biomedical applications in particular.[15, 16, 17] Electrospun polyurethane nanofibers have been successfully used in wound dressing thanks to an excellent oxygen permeability and barrier properties.[18] Water permeability is also important as it keeps the wound moist and prevents accumulation of fluid around the wound and on its cover. These covers perform a preventive function against infection with microorganisms, absorb blood and wound fluids to contribute to the healing process, and in some cases, to apply medical treatment to the wound[19, 20, 21].

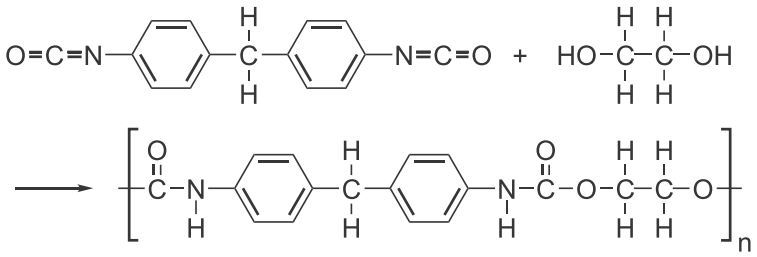

Fig. 1 Polyurethane structure

Nevertheless, there are still a lot of disadvantages and limitations of polyurethane materials, such as poor thermal capability, poor weatherability, and flammability. In order to apply PU in more fields, especially in biomedical fields, many efforts were made by combining PU and silicone together to improve those properties and break through the

limitations. To improve the properties of PU nanofibers, many efforts were made such as preparing blend nanofibers, anchoring nanoparticles, and making composites. Leonard D.Tijing et al., described the enhancing ability of electrospun polyurethane (PU) nanofibers containing carbon nanotubes (CNTs) as nanofillers for silicone film in improving the physico-mechanical properties of the composite material.[22] The incorporation of nanofibers in silicone film has also resulted to rougher surface, thus affecting the wettability of the composite film. Chan-Hee Park et al., successfully prepared the (polyurethane/nylon-6) nanofiber/ (silicone) film composites via electrospinning and dip-coating to get an obvious increase in tensile strength.[23] Silicone film has high flexibility but suffers from low tensile strength, while polyurethane film has very good tensile strength but is quite stiff. Thus, it is imperative to improve the individual properties of these polymers by either incorporating some filler materials like nanofibers or by blending different polymers.

Silicones are highly functional resins that combine the characteristics of both inorganic and organic substances and exhibit an array of useful properties including heat resistance, cold resistance, weather ability, dielectric properties, release properties and water repellency. By introducing silicones into other resins such as polyamide, polyimide, polyester, polycarbonate and polyurethane, new resin materials with enhanced functionality that includes not only heat resistance, weather ability and flame resistance, but improved impact resistance, lubricity and flexibility can be created. With their enhanced functionality, these high-performance composite resins are lightweight and have excellent fabricating characteristics and are used in a myriad of fields including electric and electronics applications, automotive applications, electrical wire, and construction.[24]

For instance, silicone-modified acrylic emulsions with hydroxyl groups may be used as automotive coatings, wood finishes, maintenance and plastic coatings.[25]

Here, we tried to get the advantages of both PU and silicone by introducing silicone groups into polyurethane polymer chains. Silicone modified polyurethane(PUSX) has attracted as useful material by various properties which combined with silicone and polyurethane, such as heat resistance, weather resistance, peeling of molding, oil resistance and high mechanical strength.[26] Currently, we use PUSX as films, molding products or adhesive, but there is no report of PUSX as fiber, in specific as nanofiber. The advantages of both polyurethane, silicone and nanofibers are very attracted to this work. We expect this new material to be applied in many fields, such as wound dressing, tissue engineering because of the biocompatibility of silicone.

1.2Literature survey

With recent developments in electrospinning, both synthetic and natural polymers can be produced as nanofibers with diameters ranging from tens to hundreds of nanometers with controlled morphology and function. The potential of these electrospun nanofibers in human healthcare applications is promising, for example in tissue/organ repair and regeneration, as vectors to deliver drugs and therapeutics, as biocompatible and biodegradable medical implant devices, in medical diagnostics and instrumentation, as protective fabrics against environmental and infectious agents in hospitals and general surroundings, and in cosmetic and dental applications.[27] Nanofiber scaffolds are well suited to tissue engineering as the scaffold can be fabricated and shaped to fill anatomical defects; its architecture can be designed to provide the mechanical properties necessary to support

cell growth, proliferation, differentiation, and motility; and it can be engineered to provide growth factors, drugs, therapeutics, and genes to stimulate tissue regeneration. An inherent property of nanofibers is that they mimic the extracellular matrices (ECM) of tissues and organs. The ECM is a complex composite of fibrous proteins such as collagen and fibronectin, glycoproteins, proteoglycans, soluble proteins such as growth factors, and other bioactive molecules that support cell adhesion and growth. Studies of cell-nanofiber interactions have shown that cells adhere and proliferate well when cultured on polymer nanofibers.[28-30] The technique of electrospinning is a promising direction for producing artificial tissues. This process utilizes an electrostatic field to control the formation and deposition of polymer nanofibers.[31-33] The procedure, which is technically feasible for the fabrication of filaments ranging in the nanometer to micrometer scale with a certain degree of alignment,[34, 35] is remarkably efficient, rapid and inexpensive. Synthetic polymers such as polylactic acid (PLA) and poly(lactic-co-glycolic acid) PLGA, and natural macromolecules such as collagen and fibrinogen, have been processed into fibrous non-woven scaffolds for use in tissue engineering research and have been shown to support stem cell growth and differentiation.[36-39]

Polyurethanes (PU) are present in many aspects of modern life. They represent a class of polymers that have found a widespread use in the medical, automotive and industrial fields. Polyurethanes can be found in products such as furniture, coatings, adhesives, constructional materials, fibers, paddings, paints, elastomers and synthetic skins.[40] Polyurethanes are replacing older polymers for various reasons. The United States government is phasing out chlorinated rubber in marine and aircraft and coatings because they contain environmentally hazardous volatile organic compounds.[41] Auto manufacturers

are replacing latex rubber in car seats and interior padding with PU foam because of lower density and greater flexibility.[42] Other advantages of PUs are that they have increased tensile strength and melting points making them more durable.[43] Their resistance to degradation by water, oils, and solvents make them excellent for the replacement of plastics.[44] As coatings, they exhibit excellent adhesion to many substances, abrasion resistance, electrical properties and weather resistance for industrial purposes.[45] Recently, polyurethane elastomers have been widely used as biomaterials, with applications ranging from medical devices andutilities like cardiac-assist pumps and blood bags, to chronic implants such as heart valves and vascular grafts. [46] Their superior mechanical properties and blood compatibility have favored their use and development as biomaterials, particularly as components of implanted devices.[47] Extensive research and development has resulted in polyurethanes with excellent biostability, exhibiting a combination of good mechanical properties and biocompatibility.

When polyurethanes are prepared into nanofibers, they are more frequently used in biomedical field especially wound dressings because of its good barrier properties, oxygen permeability and high mechanical properties. There are several reviews and book chapters dealing with the preparation and biomedical applications of polyurethane nanofibers. Lakshmi R. Lakshman et al., has reported the preparation of silver nanoparticles incorporated electrospun polyurethane nano-fibrous mat for wound dressing.[48] They proved the antibacterial ability of Ag nanoparticles anchored PU nanofibers. The results indicated that Ag-PU nanofibers could be an ideal choice for wound dressing because of the water absorption, antibacterial and cytocompatibility. Afeesh R.Unnithan et al., has introduced a wound-dressing material with antibacterial activity from electrospun dextran-

polyurethane nanofiber mats containing ciprofloxacin HCl.[49] The antibacterial electrospun scaffold was prepared by electrospinning of a solution composed of dextran, polyurethane and ciprofloxacin HCl (CipHCl) drug. They proved this electrospun nanofiber membrane containing antibiotic agents has been used as a barrier to prevent the post wound infections. They provided a basic understanding of the design of efficient nanofiber-based antibacterial wound dressing material.

In tissue engineering field, PU nanofibers are also selected as one of the best choices for cell culture. Chang HunLee et al., found out that human ligament fibroblasts cultured on aligned PU nanofibers had a similar morphology to ligament fibroblasts *in vivo*.[50] Rui Chen et al., reported a collagen functionalized thermoplastic polyurethane nanofibers (TPU/collagen) produced by coaxial electrospinning technique with a goal to develop biomedical scaffold.[51] The results demonstrated that coaxial electrospun composite nanofibers had the characters of native extracellular matrix and may be used effectively as an alternative material for tissue engineering and functional biomaterials.

And for drug delivery, Verreck et al., investigated the possibility of incorporating water soluble drugs (such as itraconazole and ketanserin) into hydrophobic polyurethane (PU) electrospun nanofibers for application in tropical drug administration.[52] The release of itraconazole from electrospun PU nanofibers increased gradually over 20 hours and there was no initial burst release. Ketanserin release was observed to be faster than itraconazole during the first 4 hours, after which, ketanserin released slowly over 24 hours.

1.3 Objectives

In this research, we tried to optimize the electrospinning process of silicone modified

polyurethane (PUSX) nanofibers on a lab scale device and a multinozzle pilot scale set-up, to investigate the potential and limitations of preparing PUSX nanofibrous sheets using different equipment. The morphology and diameter of the obtained fibers were studied via scanning electron microscopy (SEM). Attenuated total reflectance-Fourier transform infrared spectroscopy (ATR-FTIR) was also carried out to analyze the chemical structure of PUSX nanofibers. Before going for the in vitro cell attachment and proliferation applications, the all prepared nanofibers are analyzed in detail by various methods and compared with films. To investigate the effect of different structure (block and graft type), chain length and silicone concentration, physical properties evaluation was performed. Tensile tests were performed to investigate the mechanical properties such as tensile strength, elongation at break and Young's modulus. The water contact angle (WCA) measurement and water retention tests were carried out to determine the hydrophobicity of PUSX material. Thermal conductivity was analyzed in order to discuss the heat retention ability of PUSX nanofibers and films. In order to reveal the potential in cell adhesion and proliferation, NIH3T3 mouse embryonic fibroblasts cells were cultures on all the samples following by LDH activity. The toxicity of PUSX nanofibers and films was evaluated by using direct contact based on ISO 10993-5. We supposed that PUSX nanofibers could become an ideal alternative of PU membranes in biomedical fields by investigating the physical properties and biocompatibility.

1.4 Reference

[1] Thandavamoorthy Subbiah, et al. Electrospinning of nanofibers, Journal of Applied polymer science, Volume 96, Issue 2, pp 557-569, 2005.

[2] Viness Pillay, et al. A Review of the Effect of Processing Variables on the Fabrication of Electrospun Nanofibers for Drug Delivery Applications, Journal of Nanomaterials, Volume 2013, http://dx.doi.org/10.1155/2013/789289, 2013.

[3] X. Liu, et al. Polymeric scaffolds for bone tissue engineering, Annals of Biomedical Engineering, Volume 32, Number 3, pp 477-486, 2004.

[4] F. Yang, et al. Biomimetic calcium phosphate coating on electrospun poly(ε-caprolactone) scaffolds for bone tissue engineering, Chemical Engineering Journal, Volume 137, No. 1, pp 154-161, 2008.

[5] K. T. Shalumon, et al. Fabrication of chitosan/poly(caprolactone) nanofibrous scaffold for bone and skin tissue engineering, International Journal of Biological Macromolecules, Volume 48, No. 4, pp 571-576, 2011.

[6] Y. Wang, et al. Immobilization of lipase enzyme in polyvinyl alcohol (PVA) nanofibrous membranes, Journal of Membrane Science, Volume 309, No. 1-2, pp 73-81, 2008.

[7] P. Taepaiboon, et al. Vitaminloaded electrospun cellulose acetate nanofiber mats as transdermal and dermal therapeutic agents of vitamin A acid and vitamin E, European Journal of Pharmaceutics and Biopharmaceutics, Volume 67, No. 2, pp 387-397, 2007.

[8] S. Liao, et al. Processing nanoengineered scaffolds through electrospinning and mineralization suitable for biomimetic bone tissue engineering, Journal of the Mechanical Behavior of Biomedical Materials, Volume 1, No. 3, pp 252-260, 2008.

[9] C. H. Lee, et al. Nanofiber alignment and direction of mechanical strain affect the ECM production of human ACL fibroblast, Biomaterials, Volume 26, No. 11, pp 1261-1270, 2005.

[10] C. Y. Xu, et al. Aligned biodegradable nanofibrous structure: a potential scaffold for blood vessel engineering, Biomaterials, Volume 25, No. 5, pp 877-886, 2004.

[11] F. Yang, et al. Electrospinning of nano/micro scale poly(l-lactic acid) aligned fibers and their potential in neural tissue engineering, Biomaterials, Volume 26, No. 15, pp 2603-2610, 2005.

[12] Y. S. Zhou, et al. Electrospun water-soluble carboxyethyl chitosan/poly(vinyl alcohol) nanofibrous membrane as potential wound dressing for skin regeneration, Biomacromolecules, Volume 9, No. 1, pp 349-354, 2008.

[13] N. Bhardwaj, et al. Electrospinning: a fascinating fiber fabrication technique, Biotechnology Advances, Volume 28, No. 3, pp 325-347, 2010.

[14] Zoran S. Petrović. Polyurethanes, Handbook of Polymer Synthesis: Second Edition, CRC Press, pp 984, 2004.

[15] Rockwood DN, et al. Characterization of biodegradable polyurethane microfibers for tissue engineering, Journal of Biomaterials Science, Volume 18, pp 743-758, 2007.

[16] Zdrahala RJ, et al. Biomedical applications of polyurethanes: a review of past promises, present realities, and a vibrant future, Journal of Biomaterials Applications, Volume 14, pp 67-90, 1999.

[17] Sheikh FA, et al. Electrospun antimicrobial polyurethane nanofibers containing silver nanoparticles for biotechnological applications, Macromolecular Research, Volume 17, pp 688-696, 2009.

[18] Esra KiliçArzu, et al. Preparation of electrospun polyurethane nanofiber mats for the release of doxorubicine, Journal of Materials Science: Materials in Medicine, Volume 29, Issue 1, 2017.

[19] Lionelli GT, et al. Wound dressing, Surgical Clinics of North America, Volume 83, pp 617-38, 2003.

[20] Thomas S. Wound management and dressings, Journal of Pharmacy and Pharmacology, Volume 1, pp 37-57, 1990.

[21] Bhardwaj N, et al. Electrospinning: a fascinating fiber fabrication technique, Biotechnology Advances, Volume 28, pp 325-347, 2010.

[22] Leonard Demegilio Tijing, et al. Improved mechanical properties of solution-cast silicone film reinforced with electrospun polyurethane nanofiber containing carbon nanotubes, Applied Surface Science, Volume 264, pp 453-458, 2013.

[23] Chan-Hee Park, et al. Preparation and characterization of (polyurethane/nylon-6) nanofiber/ (silicone) film composites via electrospinning and dip-coating, Fibers and Polymers, Volume 13, Issue 3, pp 339-345, 2012.

[24] Marco Heuer. New Types of Silicone Resin Open Up Wider Fields of Application, Paint and coating industry, 2016.

[25] F. A. Zhang, et al. Application of a silicone-modified acrylic emulsion in two-component waterborne polyurethane coatings, Journal of Coatings Technology and Research, Volume 4, Issue 3, pp 289-294, 2007.

[26] Arun Anand Prabu, et al. Mechanical and Electrical Studies of Silicone Modified Polyurethane–Epoxy Intercrosslinked Networks, Polymer Journal, Volume 36, pp 848-855, 2004.

[27] SeeramRamakrishna, et al. Electrospun nanofibers: solving global issues, Materials Today, Volume 9, Issue 3, pp 40-50, 2006.

[28] Laurencin C.T, et al. Tissue Engineering: Orthopedic Applications, Annual Review of

Biomedical Engineering, Volume 1, pp 19-46, 1999.

[29] Peter X. Ma, et al. Synthetic nano-scale fibrous extracellular matrix, Journal of Biomedical Materials Research banner, Volume 46, Issue 1, pp 60-72, 1999.

[30] Andrzej Fertala, et al. Mapping critical sites in collagen II for rational design of gene-engineered proteins for cell-supporting materials, Journal of Biomedical Materials Research banner, Volume 57, Issue 1, pp 48-58, 2001.

[31] Zheng Ming Huang, et al. A review on polymer nanofibers by electrospinning and their applications in nanocomposites, Composites Science and Technology, Volume 63, Issue 15, pp 2223-2253, 2003.

[32] Audrey Frenot, et al. Polymer nanofibers assembled by electrospinning, Current Opinion in Colloid & Interface Science, Volume 8, Issue 1, pp 64-75, 2003.

[33] D. H. Reneker, et al. Electrospinning of Nanofibers from Polymer Solutions and Melts, Advances in Applied Mechanics, Volume 41, 2007.

[34] A Theron, et al. Electrostatic field-assisted alignment of electrospun nanofibers, Nanotechnology, Volume 12, Issue 3, 2001.

[35] E. Zussman, et al. Formation of nanofiber crossbars in electrospinning, Applied Physics Letters, Volume 82, No. 6, pp 973-975, 2003.

[36] R. James Koch, et al. Tissue Engineering with Chondrocytes, Facial plastic Surgery, Volume 18, Issue 1, pp 59-68, 2002.

[37] J. A. Matthews, et al. Electrospinning of Collagen Nanofibers, Biomacromolecules, Volume 3, Issue 2, pp 232–238, 2002.

[38] Gary E. Wnek, et al. Electrospinning of Nanofiber Fibrinogen Structures, Nano Letters, Volume 3, Issue 2, pp 213-216, 2003.

[39] Eugene D. Boland, et al. Electrospinning collagen and elastin: Preliminary vascular tissue engineering, Frontiers in Bioscience, Volume 9, pp 1422-1432, 2004.

[40] Gary T. Howard. Biodegradation of polyurethane: a review, International Biodeterioration & Biodegradation, Volume 49, Issue 4, pp 245-252, 2002.

[41] C.R. Hegedus, et al. A review of organic coating technology for U.S. naval aircraft, Journal of Coatings Technology, Volume 61, pp 31-42, 1989.

[42] Ulrich. H. Polyurethane. In: Modern Plastics Encyclopedia, Volume 60, pp 76-84, 1983.

[43] O. Bayer. Polyurethanes, Modern Plastics, Volume 24, pp 149-152, 1947.

[44] J.H. Saunders, et al. Polyurethanes, Chemistry and Technology, Part II: Technology, Interscience Publishers, UK, 1964.

[45] J. Urbanski, et al. Handbook of Analysis of Synthetic Polymers and Plastics, Ellis Horwood Limited, Chichester, UK, 1977.

[46] S. Gogolewski. In vitro and in vivo molecular stability of medical polyurethanes: A review, Trends in polymer science, Volume 1, pp 47-61, 1991.

[47] N.M.K. Lamba, et al. Polyurethanes in Biomedical Applications, CRC Press, pp 1-3, 1997.

[48] Lakshmi R. Lakshman, et al. Preparation of Silver Nanoparticles Incorporated Electrospun Polyurethane Nano-fibrous Mat for Wound Dressing, Journal of Macromolecular Science, Part A, Pure and Applied Chemistry, Volume 47, Issue 10, pp 1012-1018, 2010.

[49] Afeesh R. Unnithan, et al. Wound-dressing materials with antibacterial activity from electrospun polyurethane–dextran nanofiber mats containing ciprofloxacin HCl,

Carbohydrate Polymers, Volume 90, Issue 4, pp 1786-1793, 2012.

[50] Chang Hun Lee, et al. Nanofiber alignment and direction of mechanical strain affect the ECM production of human ACL fibroblast, Journal of Biomaterials, Volume 26, Issue 11, pp 1261-1270, 2005.

[51] Rui Chen, et al. Preparation and characterization of coaxial electrospun thermoplastic polyurethane/collagen compound nanofibers for tissue engineering applications, Colloids and Surfaces B: Biointerfaces, Volume 79, Issue 2, pp 315-325, 2010.

[52] Verreck G, et al. Incorporation of drugs in an amorphous state into electrospun nanofibers composed of a water-insoluble, nonbiodegradable polymer, Journal of Controlled Release, Volume 92, Issue 3, pp349-360, 2003.

Chapter 2

Synthesis of PUSX

2 Synthesis of PUSX

2.1 Aim of the synthesis

For biomedical applications, polyurethane elastomers offer superior mechanical properties over silicone elastomers, particularly in relation to tear and abrasion, and flex-fatigue life.[1] The chemical composition of these elastomers offers substantial opportunities to synthetic polymer chemists to tailor the structures to meet specific requirements. Thermoplastic polyurethane elastomers are a class of linear segmented copolymers characterised by the presence of urethane (carbamate) groups. They are prepared from three components: a diisocyanate, a macrodiol, and a chain extender,[2] and can be categorised into two major groups depending on the macrodiol used i.e. ester-based or ether-based polyurethanes.[3] Extensive research and development has resulted in polyurethanes with excellent biostability, exhibiting a combination of good mechanical properties and biocompatibility.

In this research, we performed the modification of polyurethanes, although numerous publications and patents claim polyurethane to be biocompatible and blood compatible. The reason is that some claims are exaggerated and others only applicable to specific situations. While the mechanical properties (such as toughness, flexibility, durability, fatigue resistance) of PUs meet requirements, clinical evidence is that there are problems related to PU surface properties. No currently available polyurethane achieves long-term hemocompatibility, and in contact with soft tissue there occurs a foreign body defense reaction.[4] Clearly, the occurrence of adverse reactions to PUs in various biomedical environments attests to their being “bio-incompatible” to varying extents; some appear to

promote less severe reactions than others, but all PUs are not integrated into the body in the way the clinician would wish them to be.

The aim of this modification study is to maintain the mechanical properties of polyurethanes while providing a surface with improved biocompatibility and hydrophobicity. Our synthetic approach is also been used specifically to obtain PU surfaces with desired mechanical properties.

Before us, there were several examples of polyurethane modification by incorporating different groups, especially silicone groups. An example is the work of Yoon et al in which a polydimethylsiloxane (PDMS) soft segment was used; surface analysis revealed that the surface was completely covered with this segment. There was, however, strong dependence of the surface properties on casting.[5] Another similar example of our material is PurSil™ thermoplastic silicone polyether urethane, which has been proved with biocompatibility and biostability, containing silicone as a soft segment which is prepared by incorporating polydimethylsiloxane into the polymer soft segment with polytetramethyleneoxide and the hard segment consists of an aromatic diisocyanate.[6] In our research, we synthesized the copolymer into different structures containing different segment compared with PurSil™.

2.2 Synthesis process

The PUSX resin can be obtained by the reaction of a polyol, a chain extender, an active hydrogen group containing organopolysiloxane and a polyisocyanate. The active hydrogen group containing organopolysiloxane is preferably an organopolysiloxane of the following formula:

$$R^1SiR^2R^3O(SiR^2R^3O)_nSiR^2R^3R^1$$

Here, as for R^1 group, monovalent hydrocarbon groups of 2 to 6 carbon atoms which have a primary hydroxyl group or a secondary hydroxyl group and may have on the chain an oxygen atom, and monovalent hydrocarbon groups which have a primary amino group or a secondary amino group are preferred. 2-hydroxyeth-1-yl, 3-hydroxyprop-1-yl, 3-(2-hydroxyethoxy) prop-1-yl and 3-aminoprop-1-yl groups are more preferred. And for R^2 and R^3 groups, groups selected from among methyl, phenyl, 3,3,3-trifluoropropyl and vinyl groups are preferred. n is an integer from 1 to 200, and preferably an integer from 5 to 50. Any hitherto known polyisocyanate may be used as polyisocyanate.

The carbinol-modified silicone (silicone polyol) used in the synthesis process of PUSX was hydrosilylated by organopolysiloxane (with Si-H group) and unsaturated alcohol compound, catalyzed by platinum catalyst. The synthesis of block type silicone polyol (diterminal diols) is showed in scheme 1a, graft type silicone polyol (monoterminal diols) can also be prepared by this method. Here, both R^1 and R^2 are methyl group ($-CH_3$) while R^3 is $-OC_2H_4-$ group.

Polytetramethylene glycol (polyol component: A in Scheme 1b) and 1,4-butanediol (chain extender: B in Scheme 1b) were used to form the polyurethane resin as common component. To synthesize PUSX, it is essential to add silicone polyol copolymer structures (block type and graft type) and different silicone chain lengths (the number of repeat units of dimethylsiloxane: *n*), followed by specific reaction with diisocyanate component in Scheme 1b in DMF/MEK mixed solvent. These synthesized PUSX solutions in DMF/MEK standardized a solid content of 30wt%. The structures of two types of PUSX are showed in Fig. 2.

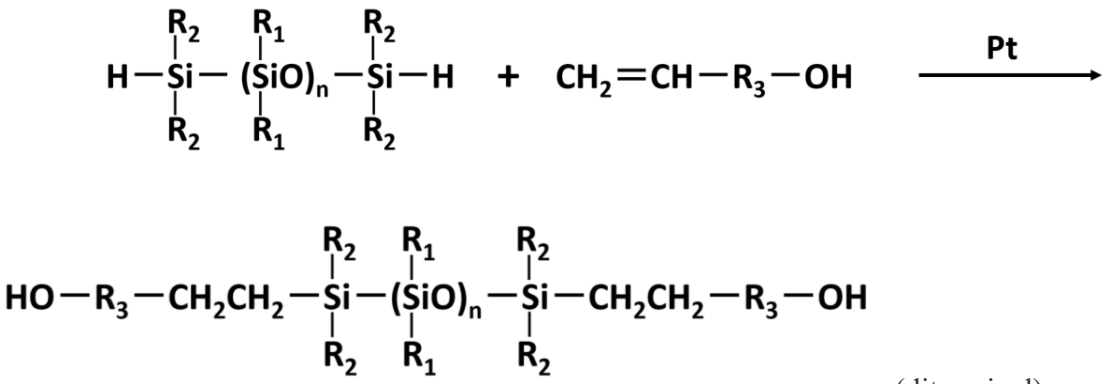

OR

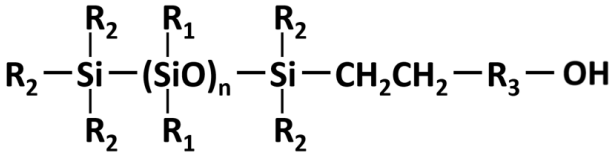

Scheme 1a. Synthesis method of carbinol-modified silicone (silicone polyol).

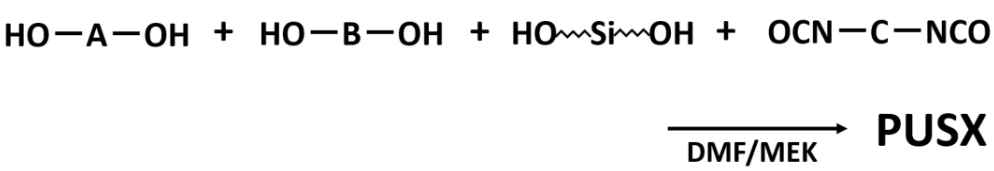

Scheme 1b. Synthesis method of PUSX.

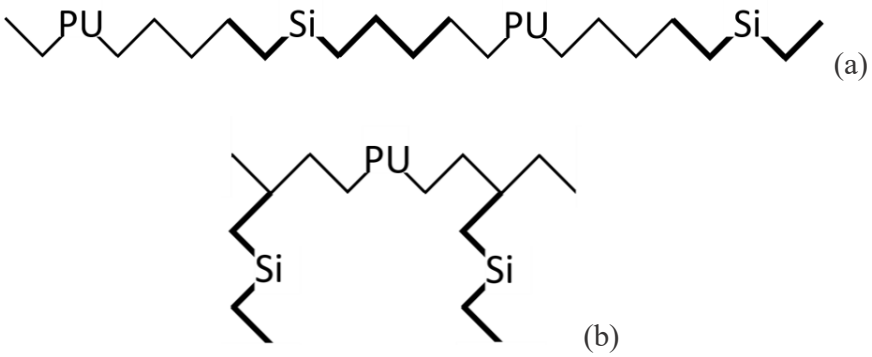

Fig. 2. Structures of block type PUSX (a) and graft type PUSX (b).

For example, in order to prepare PUSXSi01 samples, a reactor quipped with a stirrer, a reflux condenser, a thermometer and a nitrogen inlet and having also an open neck was furnished for use. While purging the reactor interior with nitrogen gas, the reactor was charged with 200g of polytetramethylene glycol, 38g of 1,4-butanediol, 45g of a diterminated silicone diol and 676.5g of dimethylformamide (DMF). Stirring under applied heat was begun, after the interior of the system had become uniform, 168.0g of 4,4'-methylenebis (phenylene isocyanate) (MDI) was added at 50℃, following which the temperature was raised to 80℃, thereby effecting the reaction. The reaction was made to proceed until the absorption at 2270cm^{-1} attributable to free isocyanate groups, as measured by infrared absorption spectroscopy, disappeared. Next, 60.1g of DMF and 315.7g of methyl ethyl ketone (MEK) were added, thereby giving the silicone polyurethane resin having a silicone content of 10.0%, a number-average molecular weight (M_n) of 73,000 and a solid content of 30%. The other 11 samples were synthesized in the similar way by changing the diterminated silicone diamine compound (n=10~120) or the amount of diterminated silicone diol.

2.3 References

[1] M. J. Wiggins, et al. Effect of strain and strain rate on fatigue-accelerated biodegradation of polyurethanes, Journal of Biomedical Materials Research, Volume 66, pp 463-475, 2003.

[2] P. A. Gunatillake, et al. Designing biostable polyurethane elastomers for biomedical implants, Australian Journal of Chemistry, Volume 56, pp 545-557, 2003.

[3] K. Knoerr, et al. Millable polyurethane elastomers, Handbook of Elastomers (2nd ed.),

Marcel Decker, Inc., New York, pp 753-764, 2001.

[4] Patrick Vermette, et al. Biomedical Applications of Polyurethanes, Tissue Engineering Intelligence Unit, 1st Edition, CRC Press, US, 2001.

[5] Sung Chul Yoon, et al. Surface and bulk structure of segmented poly (ether urethanes) with perfluoro chain extenders. 5.incorporation of poly (dimethylsiloxane) and polyisobutylene macroglycols, Macromolecules, Volume 27, Issue 6, pp 1548-1554, 1994.

[6] Narendra Pal Singh Chauhan, et al. Polyurethanes: Silicone–Polyurethane Copolymers, Encyclopedia of Biomedical Polymers and Polymeric Biomaterials, CRC Press, US, 2015.

Chapter 3

Electrospinning of PUSX nano-fibers: Mapping the parameters

3 Electrospinning of PUSX nanofibers: Mapping the parameters

3.1 Introduction

Nanofibers are defined as fibers with diameters less than 100 nanometers. In the textile industry, this definition is often extended to include fibers as large as 1000 nm diameter. They can be produced by melt processing, interfacial polymerization, electrospinning, antisolvent-induced polymer precipitation and electrostatic spinning. Electrospinning is a fiber production method which uses electric force to draw charged threads of polymer solutions or polymer melts up to fiber diameters in the order of some ten nanometers. Electrospinning shares characteristics of both electrospraying and conventional solution dry spinning of fibers. The process does not require the use of coagulation chemistry or high temperatures to produce solid threads from solution. This makes the process particularly suited to the production of fibers using large and complex molecules. Electrospinning from molten precursors is also practiced; this method ensures that no solvent can be carried over into the final product. The size of an electrospun fiber can be in the nano scale and the fibers may possess nano scale surface texture, leading to different modes of interaction with other materials compared with macroscale materials. In addition to this, the ultra-fine fibers produced by electrospinning are expected to have two main properties, a very high surface to volume ratio, and a relatively defect free structure at the molecular level. This first property makes electrospun material suitable for activities requiring a high degree of physical contact, such as providing sites for chemical reactions, or the capture of small sized particulate material by physical entanglement-filtration. The second property should allow electrospun fibers to approach the theoretical maximum

strength of the spun material, opening the possibility of making high mechanical performance composite materials.

Electrospun nanofibers (NFs) have attracted much attention due to their unique properties such as large surface area to volume ratio, biocompatibility, simple surface functionalization, easy handling and outstanding mechanical properties.[1-3] Nanofibers, with their large surface-to-volume ratio, have the potential for use in various applications where high porosity is desirable. A porous structure made from nanofibers is a dynamic system where the pore size and shape can change, unlike conventional rigid porous structures. Nanofibers can also be linked to form a rigid structure if required. Perhaps the most versatile process for producing nanofibers with relatively high productivity is electrospinning.[4] Porous nanofiber meshes made by electrospinning have been identified for use in numerous applications as shown in Fig. 3.

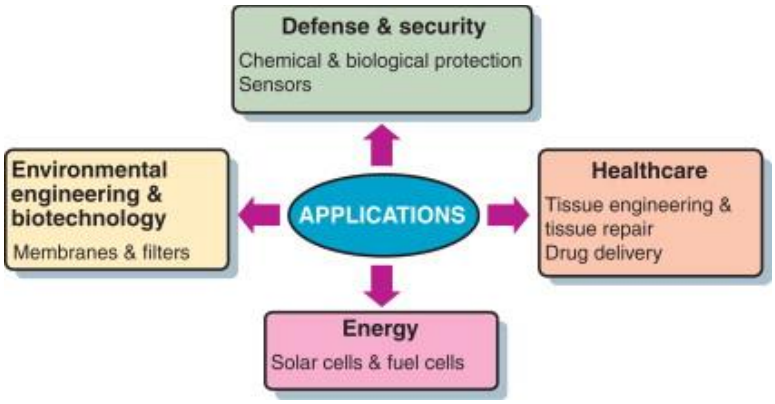

Fig. 3. Various applications of nanofibers in recent years.

Electrospun nanofibers including polyurethane nanofibers have attracted much attention due to their unique properties such as very large surface area to volume ratio, flexibility in surface functionalities, superior mechanical performance, high porosity, and good

interfacial adhesion.[4-5] PU nanofibers were perfectly prepared and studied by a large amount of researchers in recent years. For instance, Haitao Zhuo et al. discussed the influence of electrospinning parameters including the applied voltage, feeding rate, and solution concentration on the diameters and morphology of PU nanofibers[6] while F. Cengiz et al. investigated the effect of tetraethyl ammonium bromide salt on the spinnability of PU nanofibers.[7] S. Thandavamoorthy et al. discovered the self-assembling phenomenon in electrospun PU nanofibers.[8] However, PUSX nanofibers are not that easy to prepare because of the existence of silicone. To make silicone into electrospun nanofibers, several ways were reported by researchers. Haitao Niu et al. suggested a modified core–shell electrospinning method using a commercially available liquid polydimethylsiloxane (PDMS) precursor and polyvinylpyrrolidone (PVP) as core and sheath materials to prepare continuous ultrafine PDMS fibers with an average diameter around 1.35 μm.[9] After removing PVP by dissolving method, the PDMS fiber surface was not as ideal as expected. Ruiping Xue et al. also tried the core-shell electrospinning method to prepare PDMS core-polycaprolactone (PCL) shell nanofibers for biocompatible, real-time oxygen sensor applications.[10] Since the PDMS core was very viscous, the existence of thin PCL shell became essential to maintain the morphology. Both of them showed some limitations of the core-shell structure silicone nanofibers. Miriam Haerst et al. showed a fast crosslink way to prepare PDMS nanofibers by electrospinning PDMS-acetone solutions on a 100℃ heat plate. Unfortunately, the average diameter appeared to be large compared to other electrospun polymer nanofibers.[11] On the other hand, nanofibers made from silicone resins have been reported,[12] organopolysiloxane fibers with diameters ranging from 0.01μm to 100μm were prepared by electrospinning process. Also, the electrospun silsesquioxane

nanofibers for battery separator materials were reported[13]. Unfortunately, both reports could not show the uniform nanofibers with ideal fine diameters so that the physical properties and other characteristics are still unknown.

In this chapter, we optimized the electrospinning process of PUSX nanofibers on a lab scale device and discussed the influence of polymer solution concentration, solvent ratio and environment conditions on the electrospinning process.

3.2 Materials

All the 12 kinds of silicone modified polyurethane (PUSX) solutions were kindly synthesized using the method discussed in chapter 2 by Shin-Etsu Chemical Co., Ltd and Dainichiseika Color & Chemicals Mfg. Co., Ltd. The weight average molecular weight (M_w) is a polymethyl methacrylate (PMMA) equivalent value measured by gel permeation chromatography (GPC). GPC measurements were carried out with an HLC-8320 GPC system (Tosoh Corporation, Japan), tetrahydrofuran (THF) as the solvent, and at a resin concentration 0.1%. Defined PUSX with M_w ranging from 1.48×10^5 to 2.33×10^5 were synthesized. Solvents such as *N, N*-dimethylformamide (DMF) and ethyl methyl ketone (MEK) were purchased from Wako Pure Chemical Industries., Ltd and used as received.

3.3 Electrospinning devices

Several processing techniques such as drawing[14], template synthesis[15], phase separation[16], self-assembly[17], electrospinning[18], melt blowing[19], etc. have been used to prepare polymer nanofibers in recent years. The drawing is a process like dry spinning in fiber industry, which can make one-by-one very long single nanofibers. However, only a viscoelastic

material that can undergo strong deformations while being cohesive enough to support the stresses developed during pulling can be made into nanofibers through drawing. The template synthesis, as the name suggests, uses a nanoporous membrane as a template to make nanofibers of solid (a fibril) or hollow (a tubule) shape. The most important feature of this method may lie in that nanometer tubules and fibrils of various raw materials such as electronically conducting polymers, metals, semiconductors, and carbons can be fabricated. On the other hand, the method cannot make one-by-one continuous nanofibers. The phase separation consists of dissolution, gelation, extraction using a different solvent, freezing, and drying resulting in a nanoscale porous foam. The process takes relatively long period of time to transfer the solid polymer into the nano-porous foam. The self-assembly is a process in which individual, pre-existing components organize themselves into desired patterns and functions. However, similarly to the phase separation the self-assembly is time-consuming in processing continuous polymer nanofibers. Thus, the electrospinning process seems to be the only method which can be further developed for mass production of one-by-one continuous nanofibers from various polymers.[19]

Fig.4 shows a schematic illustration of the basic setup for electrospinning. It consists of three major components: a high-voltage power supply, a spinneret (a metallic needle) and a collector (a grounded conductor). Direct current (DC) power supplies are usually used for electrospinning although the use of alternating current (AC) potentials is also feasible.[20] The spinneret is connected to a syringe in which the polymer solution is hosted. With the use of a syringe pump, the solution can be fed through the spinneret at a constant and controllable rate. When a high voltage (usually in the range of 1 to 30 kV) is applied, the pendent drop of polymer solution at the nozzle of the spinneret will become highly

electrified and the induced charges are evenly distributed over the surface. In the electrospinning process, the polymer solution held by its surface tension at the end of a capillary tube is subjected to an electric field. Charge is induced on the liquid surface by an electric field. Mutual charge repulsion causes a force directly opposite to the surface tension. As the intensity of the electric field is increased, the hemispherical surface of the solution at the tip of the capillary tube elongates to form a conical shape known as the Taylor cone.[21] When the electric field reaches a critical value at which the repulsive electric force overcomes the surface tension force, a charged jet of the solution is ejected from the tip of the Taylor cone. Since this jet is charged, its trajectory can be controlled by an electric field. As the jet travels in air, the solvent evaporates, leaving behind a charged polymer fiber which lays itself randomly on a collecting metal screen. Thus, continuous fibers are laid to form a non-woven fabric.[22]

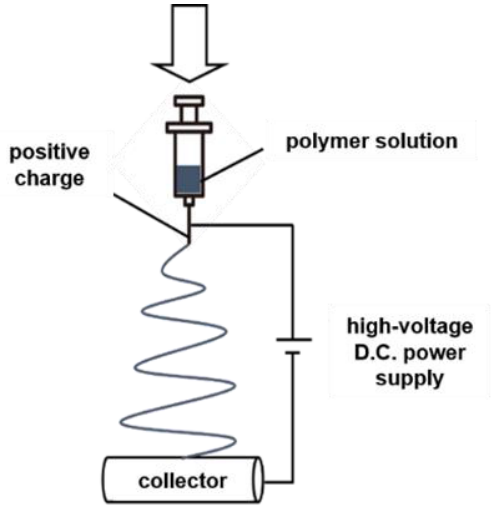

Fig. 4. Schematic illustration of the basic setup for electrospinning.

In this chapter, to explore the electrospinnabiliy of PUSX and map the parameters, horizontal mononozzle lab scale device (NEU Nanofiber Electrospinning Unit, Kato Tech Co., Ltd, as shown in Fig. 5) was used. Tips of metal injection needles (ø0.6mm, length 26mm) were cut before being used and placed 30^{o} to the floor. Lab scale air compressor (HITACHI POD-2, 2MNA6), adsorption air dryer (QSQ020A, Higashinihon Orion Co., Ltd) and micro flow rate temperature and humidity control apparatus (Kotohira, KTC-Z15A 1501) were applied to optimize the humidity and temperature.

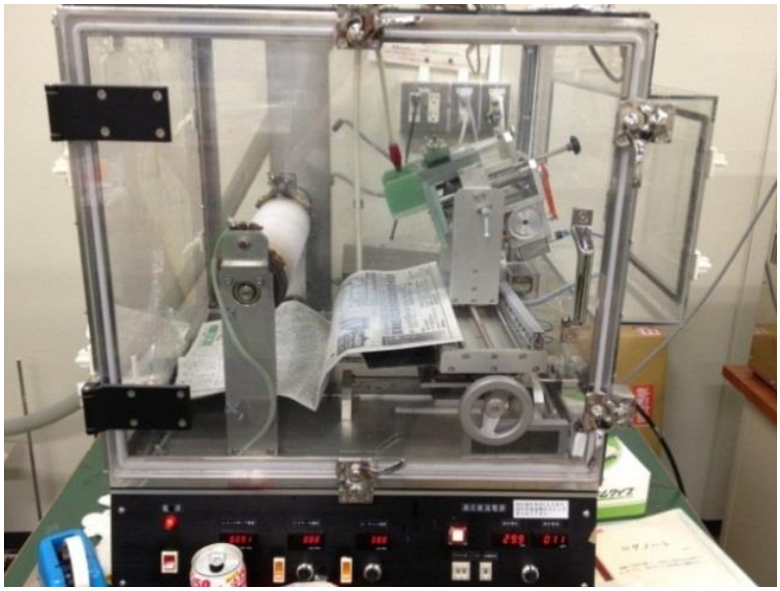

Fig. 5. The lab scale electrospinning set-up.

3.4 Electrospinning parameters

The morphology and diameter of electrospun fibers are dependent on a number of processing parameters that include: a) the intrinsic properties of the solution such as the type of polymer, the conformation of polymer chain, viscosity (or concentration), elasticity, electrical conductivity, and the polarity and surface tension of the solvent; and b) the

operational conditions such as the strength of applied electric field, the distance between spinneret and collector, and the feeding rate for the polymer solution.[23] In addition to these variables, the humidity and temperature of the surroundings may also play an important role in determining the morphology and diameter of electrospun nanofibers.[24]

In this research, various electrospinning solutions were prepared by diluting the PUSX solutions (30 wt%) in DMF/MEK mixed solvent and stirring at room temperature for 48 hours in order to obtain homogeneous solutions. To investigate the optimized parameters, all electrospinning experiments were performed by mononozzle lab scale device at room temperature (22℃) and the deposited nanofibers were collected on a drum shape rotating metallic collector. A 10-20kV voltage was applied while needle tip to collector distance was 10cm with the irradiation angle of 30^{o} and air flow rate in spinning environment was 0.1mL/min. The detailed relevant electrospinning parameters applied for each sample are discussed in 3.6.

3.5 Characterization of applied polymer solutions and prepared nanofibers

3.5.1 Viscosity measurements

The apparent viscosity of the polymer solutions with different concentrations was measured using a digital rotational viscometer (Toki Sangyo Co., Ltd. TVB-10M). As shown in Fig. 6, motor rotation is transmitted to the rotor via a torsion wire. Viscous torque acts on the rotor turning in the measured fluid. The torsion wire rotates with the wire in a deflected state at an angle which is proportional to the size of the viscous torque. The angle of deflection of the torsion wire is the same as the reciprocal deflection of slit discs A and

B which are attached to the ends of the torsion wire. Each slit disc's photo sensor read the deflection angel of the disc and this information is converted into a viscosity measurement which is displayed. A magnetic bearing positioned at the lower part of the torsion wire provides non-contact support of the rotor spindle. A software was used for the complete external control of the viscometer. Before the measurements, the viscometer was calibrated with standard oil (1000 mPa*s and 10000 mPa*s, standardized by Cannon-Fenske Viscometer), and the computed maximum uncertainty in the viscosity measurement was lower than 5%.

(a)

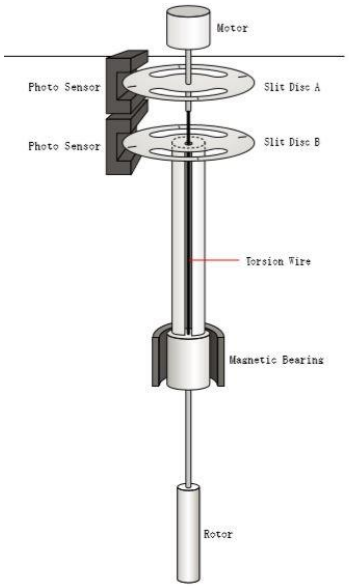

(b)

Fig. 6. (a)The digital rotational viscometer (Toki Sangyo Co., Ltd. TVB-10M) and (b) Schematic principle of operation.[25]

The measurement of the surface tension of the solution was performed by a simple surface and interfacial tensiometer (Kyowa Interface Science Co., Ltd. DY-500, as shown in Fig. 7a). The Wilhelmy plate method was employed. It is like the du Noüy ring method, but it

is simpler and does not require the correction. In this method, the plate is oriented perpendicular to the interface, and the force exerted on it is measured. When measuring unit (Wilhelmy plate) contacts the surface of the liquid, the liquid will wet the Wilhelmy plate upwards as shown in Fig. 7b. In this case, the surface tension acts along the perimeter of the plate and the liquid pulls in the plate. This method detects the pulling force is read and determines the surface tension. The instrument was computer controlled, and it was calibrated with a known weight of 400mg. The results we collected were the average of more than 3 specimens of each sample with the computed maximum uncertainty lower than 5%. For both viscosity and surface tension measurement, the number of replicates tested for each solution was 3.

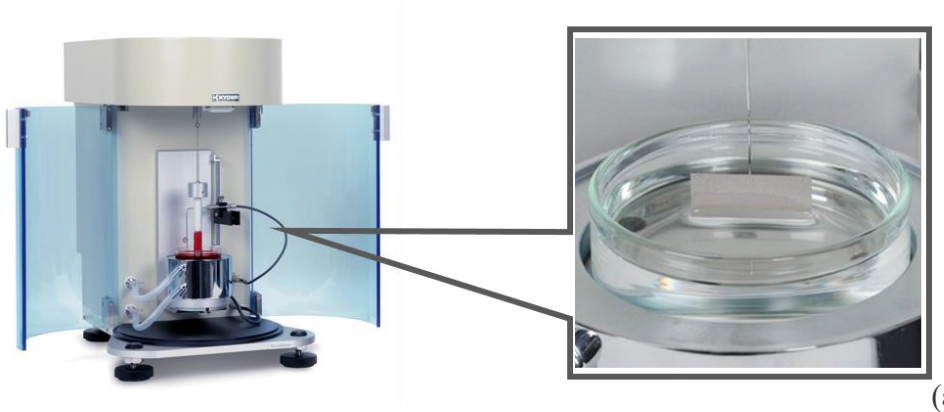

(a)

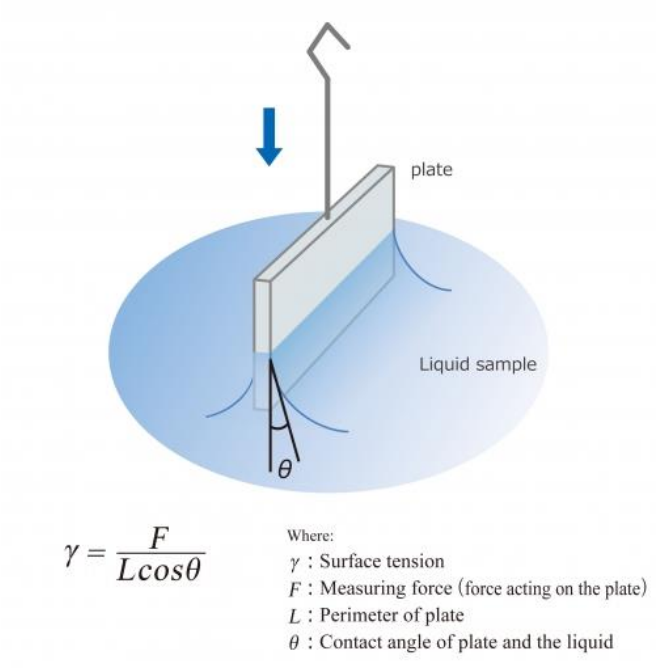

(b)

Fig. 7. (a) Surface and interfacial tensiometer (Kyowa Interface Science Co., Ltd. DY-500) and (b) Schematic illustration of Wilhelmy Plate method.[26]

3.5.2 Characterization

The first step of a scientific evaluation is to thoroughly observe the form of the material. For this purpose, we have a magnifying glass or an optical microscope. But, if light is used, we can't see anything smaller than the wavelength of light and therefore observing a nano structure is extremely difficult. The Scanning Electron Microscope (SEM) introduced here utilizes an electron beam whose wavelength is shorter than that of light and therefore observing a structure down to several nm in scale becomes possible. The Scanning Electron Microscope, which is utilized in various fields such as medical, biological, metals, semiconductors and ceramics, is broadening its application frontier. With abundant attachments and devices being combined, its capability is expanding. SEM is regarded as

one of the most powerful tools being used at R&D institutes and quality control inspection sites all over the world.

In this research, the surface morphology of nanofibers was also investigated by scanning electron microscope (SEM, JSM-6010LA JEOL, Japan, as shown in Fig. 8a) at an accelerating voltage of 10 kV. The prepared sample before SEM analysis was coated using a platinum sputter coater (Ion sputter JFC-1600 JEOL, Japan) under 30 mA and 30 seconds to be observed by SEM. The diameters of nanofibers were measured by Image J (National Institutes of Health, US). The average fiber diameters and their standard deviations were calculated from data of at least 50 measurements per sample.

A schematic representation of an SEM is shown in Fig. 8b. Electrons are generated at the top of the column by the electron source. They are then accelerated down the column that is under vacuum, which helps to prevent any atoms and molecules present in the column from interacting with the electron beam and ensures good quality imaging. Electromagnetic lenses are used to control the path of the electrons. The condenser defines the size of the electron beam (which defines the resolution), while the objective lens' main role is the focusing of the beam onto the sample. Scanning coils are used to raster the beam onto the sample. In many cases, apertures are combined with the lenses in order to control the size of the beam. Different types of electrons are emitted from samples upon interacting with the electron beam. A Back Scattered Electron detector is placed above the sample to help detect backscattered electrons. Images show contrast information between areas with different chemical compositions as heavier elements (high atomic number) will appear brighter. A Secondary Electron detector is placed at the side of the electron chamber, at an angle, in order to increase the efficiency of detecting secondary electrons which can

provide more detailed surface information.

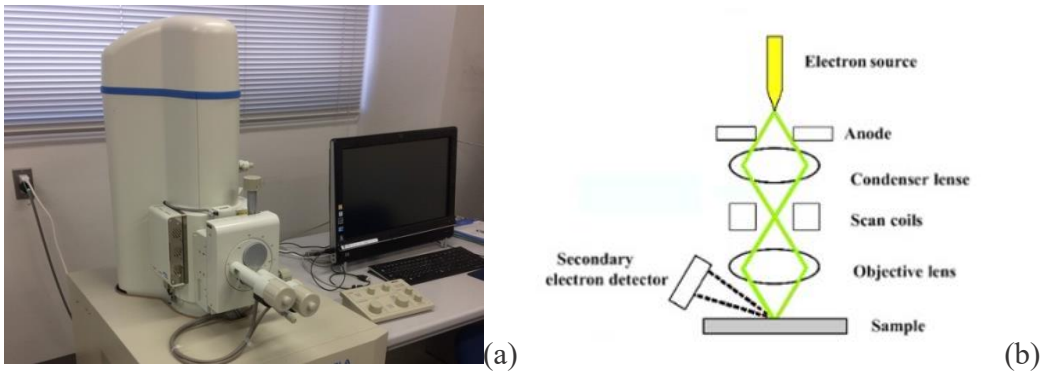

(a) (b)

Fig. 8. (a) Scanning Electron Microscope (SEM, JSM-6010LA JEOL) and (b) schematic illustration of SEM.[27]

3.6 Electrospinning of PUSX solutions (optimizations of electrospinning process)

The electrospinning process is influenced by many parameters that consecutively also affect the morphology and the diameter of the obtained fibers. These parameters can be subdivided into polymer related and processing parameters. The predominant polymer related parameters including the molecular weight, polymer concentration and the solution viscosity were varied as shown in Table 1.

From Table 1, we can see that the surface tension decreased with the increase of both silicone chain length and silicone concentration while the viscosity decreased only with the increase of silicone concentration in block type PUSX materials. Furthermore, the processing parameters such as the applied voltage, the flow rate and the needle to collector distance were adjusted in order to optimize the electrospinning process.

In the first part of this work, the influence of the polymer concentration, applied voltage,

viscosity on the fiber diameter was studied. Then, the optimized electrospinning parameters were transferred to a multinozzle pilot scale set-up to investigate the reproducibility of the fiber production method, the transferability of the electrospinning parameters and the feasibility of upscaling the procedure.

Table 1. PUSX samples of block type (Si01, Si02, Si03, Si04, Si01-20, Si01-40, Si01-59) and graft type (Si05, Si06, Si07, Si08). (n = 3)

	Silicone concentration (wt%)	Silicone chain length (n)	M_w ($\times 10^5$)	M_n ($\times 10^5$)	Viscosity (15wt%, mPa*s)	Surface tension (mN/m)
PU	0	×	1.48	0.75	700	33.4
Si01	10	20	1.69	0.87	635	24.2
Si02	10	10	1.39	0.73	328	25.5
Si03	10	30	1.59	0.79	378	23.9
Si04	10	50	1.66	0.75	412	24.1
Si01-20	20	20	1.74	0.88	616	23.0
Si01-40	40	20	2.01	1.02	443	22.2
Si01-59	59	20	2.33	1.11	219	21.8
Si05	10	10	1.56	0.71	520	25.0
Si06	10	25	1.61	0.70	720	19.1
Si07	10	30	1.57	0.72	810	23.6
Si08	10	120	1.62	0.78	820	24.7

3.6.1 Effect of polymer concentration

The electrospinning process relies on the phenomenon of the uniaxial stretching of a charged jet. The stretching of the charged jet is significantly affected by changing the concentration of the polymeric solution.[28] For example when the concentration of the polymeric solution is low, the applied electric field and surface tension cause the entangled polymer chains to break into fragments before reaching the collector.[29] These fragments cause the formation of beads or beaded nanofibers. Increasing the concentration of the polymeric solution will lead to an increase in the viscosity, which then increases the chain entanglement among the polymer chains. These chain entanglements overcome the surface tension and ultimately result in uniform beadless electrospun nanofibers. Furthermore, increasing the concentration beyond a critical value hampers the flow of the solution through the needle tip (the polymer solution dries at the tip of the metallic needle and blocks it), which ultimately results in defective or beaded nanofibers.[30] The morphologies of the beads depict an interesting shape change from a round droplet-like shape (with low-viscosity solutions) to a stretched droplet or ellipse to smooth fibers (with sufficient viscosity) as the solution viscosity changes.[31] It can be concluded that the solution concentration is one of the most significant parameters for electrospinning and affects the viscosity. Electrospinning of polymer solutions with too low concentrations results in the formation of beads and heterogeneous fibers, and upon increasing concentration their shape evolves from spheres to spindles until uniform fibers are produced at the appropriate concentration. Conversely, high concentration leads to too viscous solutions for which continuous flow cannot be maintained, leading to electrospinning instability and the formation of thick and inhomogeneous fibers. Thus, an optimal concentration range for the

electrospinning of polymers, resulting in stable and reproducible fiber production must be determined. In this research, the optimal range for successful electrospinning of all the different PUSX fibers was around 10wt%~20wt% according to Table 3.

Table 2 shows the SEM morphologies of electrospun block type and graft type PUSX fibers with solution concentrations range of 0~10wt%, 10~15wt%, and 15~20wt%. At higher concentration, the presence of PUSX polymer is much more than that at lower concentration, resulting in enhanced interaction and entanglement of chains to resist deformation. For Si01 and Si02 nanofibers, the number of beads decreased with increasing polymer concentration, and eventually became uniform fibers. Irregular beads were formed because the very low viscosity did not suffice to sustain the elongation of the liquid jet, and therefore the thin jet of solution left the nozzle instantly and shrunk to droplets. For Si03, Si04, Si01-20, Si01-40, Si01-59 nanofibers, low concentration leads to irregular beads, but too high concentration also leads to too viscous solutions for which continuous flow cannot be maintained. Especially for Si01-40 and Si01-59, uniform and continuous nanofibers cannot be formed when the polymer concentration is higher than 10wt% because the ratio of silicone to PU is much higher in Si01-40 and Si01-59 than in other block type PUSX materials. Because of the electric insulting effect of silicone groups, as the polymer concentration increased, the electrostatic repulsion became more and more difficult, which explained the difficulties of the electrospinning process. In this case, the higher polymer concentration led to larger diameter of nanofibers and a shorter spinning time less than 30 minutes (* in Table 2). For graft type PUSX nanofibers, the silicone groups on the side chains cannot influence the structure too much which makes the spinnability very similar to PU nanofibers.

Table 2. SEM morphologies of the electrospun PUSX nanofibers with various structures and concentrations. (Magnification: 2000, DMF/MEK=64:36, Ø is the average diameter (nm) of each sample.)

Concentration (wt%)	PU	Si01	Si02	Si03
0~10	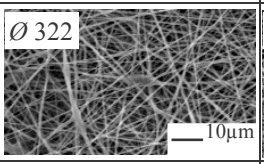	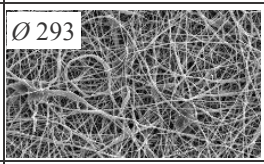	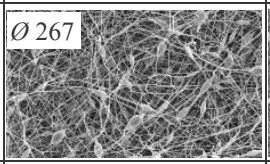	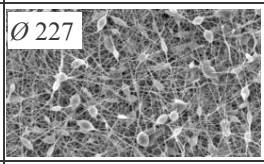
10~15	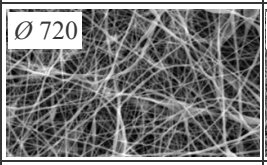	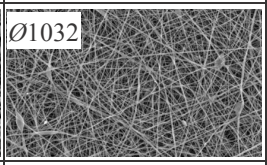	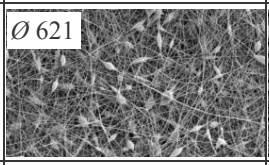	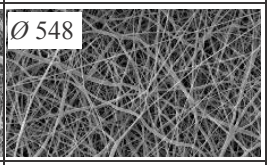
15~20	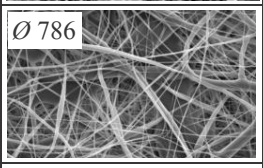	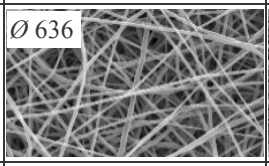	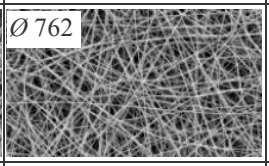	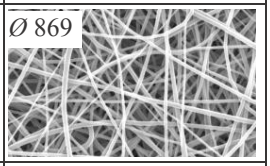
Concentration (wt%)	**Si04**	**Si01-20**	**Si01-40**	**Si01-59**
0~10	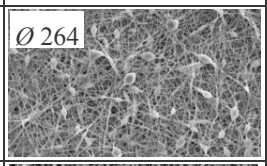	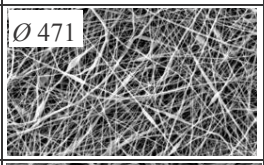	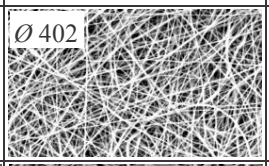	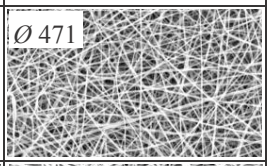
10~15	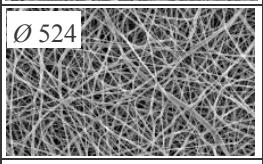	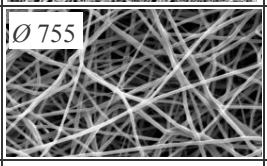	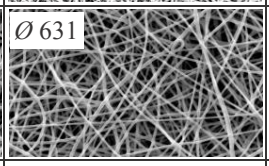	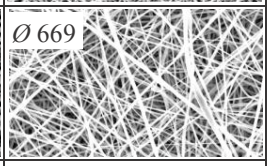
15~20	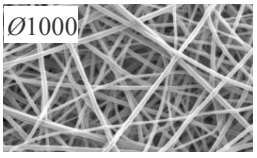	*	*	*
Concentration (wt%)	**Si05**	**Si06**	**Si07**	**Si08**
0~10	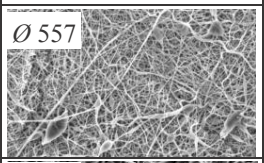	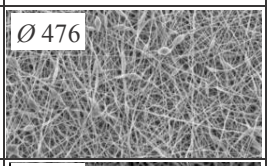	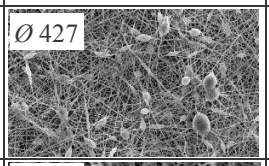	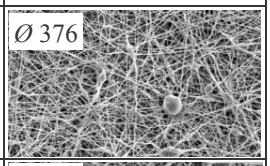
10~15	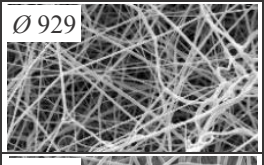	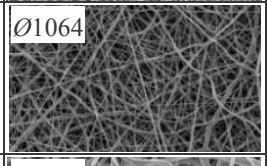	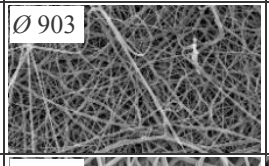	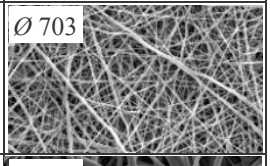
15~20	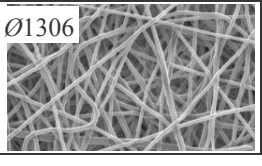	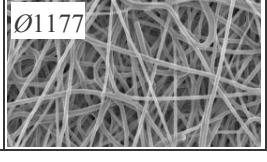	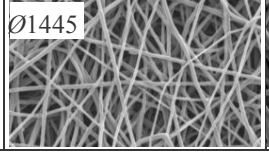	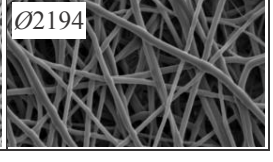

3.6.2 Effect of different solvent ratio

Another significant factor that influenced the electrospinning process a lot is the selection of solvents. Usually two things need to be kept in mind before selecting the solvent. First, the preferred solvents for electrospinning process have polymers that are completely soluble. Second, the solvent should have a moderate boiling point. Its boiling point gives an idea about the volatility of a solvent. Generally volatile solvents are fancied as their high evaporation rates encourage the easy evaporation of the solvent from the nanofibers during their flight from the needle tip to collector. However, highly volatile solvents are mostly avoided because their low boiling points and high evaporation rates cause the drying of the jet at the needle tip. This drying will block the needle tip, and hence will hinder the electrospinning process. Similarly, less volatile solvents are also avoided because their high boiling points prevent their drying during the nanofiber jet flight.[29] The deposition of solvent-containing nanofibers on the collector will cause the formation of beaded nanofibers.[32] Numerous research groups have studied the effects of the solvent and solvent system on the morphology of nanofibers and concluded that similar to the applied voltage, the solvent also affects the polymer system.[33] Furthermore, the solvent also plays a vital role in the fabrication of highly porous nanofibers. This may occur when a polymer is dissolved in two solvents: one of the solvents will act as a non-solvent. The different evaporation rates of the solvent and non-solvent will lead to phase separation and hence will result in the fabrication of highly porous electrospun nanofibers. Megelski et al. prepared porous nanofibers by varying the ratio of tetrahydrofuran (THF) and dimethylformamide (DMF).[34] In addition to the volatile nature of the solvent, its conductivity and dipole-moment are also very important.

In this study, in order to dissolve PUSX to get an easier electrospinning process, instead of using single solvent DMF, different types of solvents for electrospinning were prepared by using a mixture of DMF and MEK in the weight ratios of 64/36, 70/30, 80/20 and 90/10 in 13% (w/v) polymer concentration. PUSX Si01-20 samples were dissolved in the given solvents at room temperature (25 ± 2 °C) with 48h stirring to obtain homogeneous solutions. Fig. 9 presents the fiber morphology variation with a decreasing amount of MEK in the mixture of DMF/MEK, all the 4 samples show the fine fiber distributions. When the concentration of MEK was decreased from 30% to 10%, the diameters gradually decreased to 239nm. This could be related to insufficient resistance of the electrospinning solutions to resist electrical force stretching caused by viscosity, surface tension of the solutions, the hydrophobicity of the polymer and the boiling point of the solvent.[35] The solvent DMF has a higher boiling point of 152.8 °C than MEK (79.6 °C), and the viscosity and surface tension of the solutions decreased with the ratio of DMF/MEK. It is known that increasing the amount of MEK in the solution can decrease the charge density and electrostatic repulsion due to its lower conductivity (2×10^{-5}S/m) than that of DMF (2.5×10^{-4}S/m), leading to a trend of stable flow of the solution, stable whipping, stable Taylor cone and improvement of the fiber quality during electrospinning. While increasing the amount of DMF, the stretching of the solution jet was increased as a result of higher level of charges carried by the solution. The same factor also encourages the reduction of fiber diameter.[36] Meanwhile, higher weight percentage of DMF in the mixed solvent also attributes to unsmooth surface of nanofibers because of the slow evaporation rate. Unstable electrospinning process appeared with the increase of DMF in the mixed solvents. We could even see the existence of some beads and thinner fibers in Fig. 9 (b), (c) and (d). To

avoid rough surface and beads, we prefer to choose the ratio 64:36 (DMF: MEK) to get more uniform fibers. This experiment was also performed on PUSX Si01 and Si05 samples, similar results were obtained.

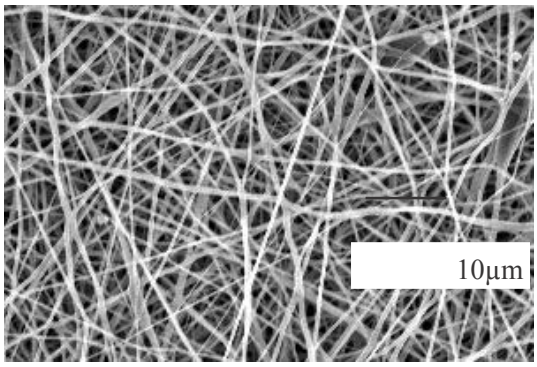

(a)

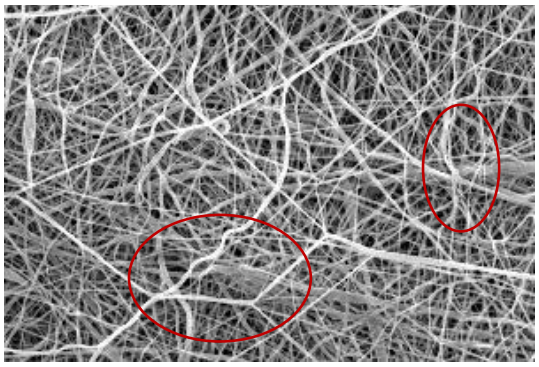

(b)

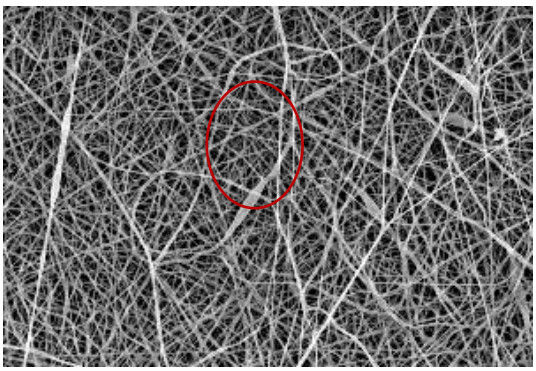

(c)

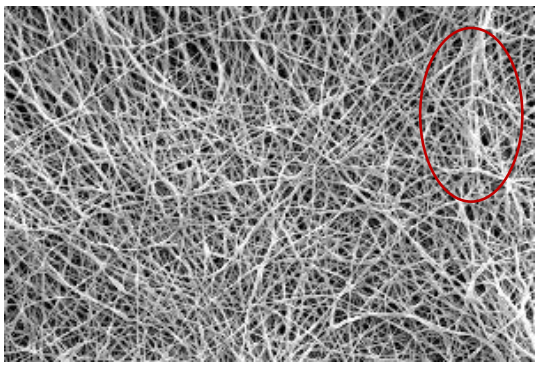

(d)

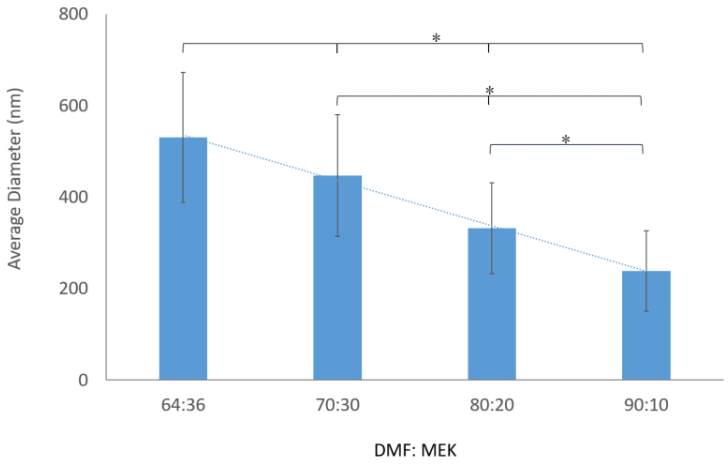

(e)

Fig. 9. SEM images of PUSX Si01-20 nanofibers under different solvent ratios. (a) 64/36, (b) 70/30, (c) 80/20, (d) 90/10 of DMF/MEK. (Magnification: 2000) (e) Average diameters of PUSX Si01-20 nanofibers with different ratio of DMF/MEK. "*" was statistically significant ($p < 0.05$) between each 2 samples.

3.6.3 Effect of different temperature

Although temperature is a key parameter in electrospinning, the related reports are extremely limited, which is possibly correlated with the simple implementation of electrospinning under ambient conditions. The key in running elevated temperature electrospinning lies in heating and maintaining the working fluid at a constant temperature different from ambient conditions.[37] According to Oliver Hardick et al' study, the atmospheric conditions most suitable for cellulose acetate nanofiber production are 25.0 °C and 50% RH, which gives the highest level of fiber diameter uniformity, the lowest level of beading and maintains a low fiber diameter for increased surface area and increased pore size homogeneity.[38] Moreover, Ji Zhou et al. suggested that for PU nanofibers, the Young's modulus decreases linearly with the increase in temperature in the range of 25 °C-60 °C.[39] In this experiment, the environment conditions such as temperature has also been optimized by PUSX Si01 materials in 10wt% solution at varying temperatures from 25 °C-60 °C.

As shown in Fig. 10, the higher temperature leads to the higher speed of solution evaporation, which results in more beads of the nanofibers. In this case, the temperature is determined to be 22°C controlled by a lab scale air compressor, an adsorption air dryer and a micro flow rate temperature and humidity control apparatus.

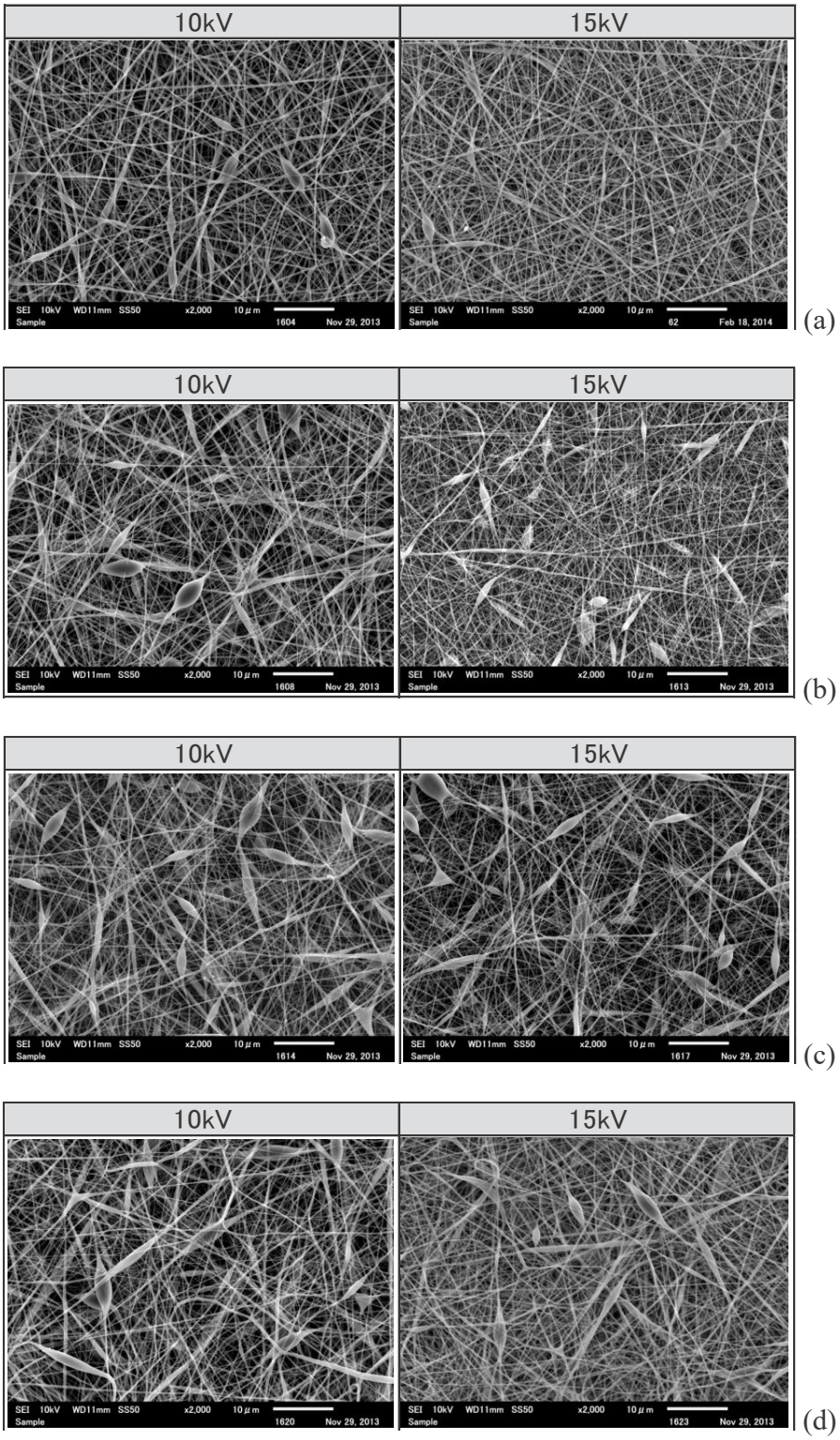

Fig. 10. SEM images of PUSX Si01 nanofibers at different temperatures. (a) 25°C, (b) 40°C, (c) 50°C and (d) 60°C. (Magnification: 2000)

3.7 Morphology of PUSX nanofibers under optimized conditions

The fiber morphology of the obtained PUSX nanofibers was studied by means of SEM. Representative SEM images of PU and block type PUSX nanofibers produced with the lab scale device are shown in Fig. 11 and Table 3.

The surface morphology of block type PUSX was smooth and continuous with fiber diameters ranging from 400 nm to 720 nm. The mean diameters of each kind of nanofibers were listed in Table 3. The mean diameters decreased with the increase of both chain length of silicone and silicone concentration. Table 4 also showed the optimized electrospinning parameters of all the 8 kinds of block type PUSX nanofibers. Beadless PU, Si01, Si02, Si03 PUSX nanofibers could only be obtained by electrospinning solutions with polymer concentrations exceeding 15wt%. The uniform fine Si04, Si01-20, Si01-40, Si01-59 PUSX nanofibers could be obtained by electrospinning with polymer concentrations lower than 13wt%. The diameters and optimized polymer concentrations of nanofibers decreased with increasing of silicone chain length because of the low surface tension. We supposed that the rather low cohesive force of silicone structure causes the low viscosity by the long silicone chain and high silicone concentration in PUSX. As a result, the optimized polymer concentrations for electrospinning were also adjusted to be low because the surface tension and viscosity highly depend on structure and concentration of silicone. Meanwhile, low polymer concentration means that the solutions contained less polymer so the diameters of nanofibers were turned out to be decreased. Different silicone chain length PUSX materials were mainly influenced by surface tension while different silicone concentration PUSX materials were mainly influenced by viscosity. This phenomenon can be explained by the

component ratio of silicone and polyurethane in PUSX. The ratio of polyurethane to silicone never change with silicone chain length while the changes happened in PUSX materials with different silicone concentrations. Compare with PU nanofibers, PUSX nanofibers shows more uniform surface with smaller diameter due to the hydrophobicity of silicone group.

Fig. 12 and Table 4 showed the surface morphologies and the optimized electrospinning parameters for graft PUSX nanofibers. To optimize the electrospinning process of graft type PUSX nanofibers, different polymer concentrations of solutions from 10wt% to 20wt% were also tried. It turned out that we can get non-uniform nanofibers with beads in the 10wt% solutions and thicker fibers in the 20wt% solutions by electrospinning. The most suitable polymer concentrations of graft type PUSX solutions for electrospinning is 15wt% (same with PU) with the mean diameters ranging from 460 nm to 560 nm. Alike, the surface morphology was fine and continuous. The diameters of nanofibers increased with the polymer concentration and there's no connection found between the silicone chain length and diameters. Compared with block type PUSX, graft type PUSX nanofibers could not show clear influence of chain length on electrospinning parameters. This might because the silicone groups on side chain are not able to influence the characters of electrospinning as much as the silicone groups on the main chain do. It may be concluded that interchain interactions and entanglement of the short side chains are too weak to make differences on the electrospinning jet.

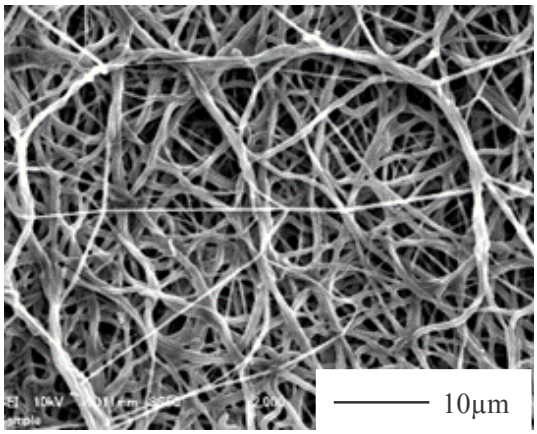

(a)

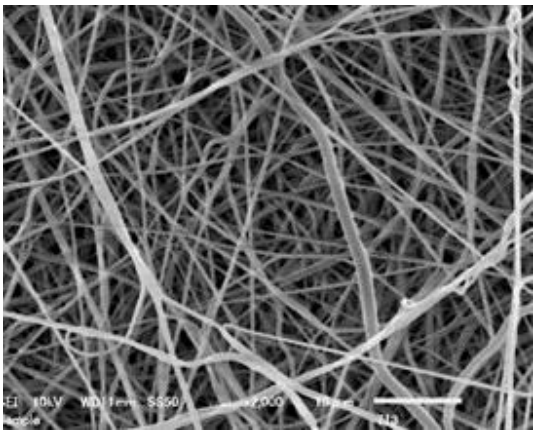

(b)

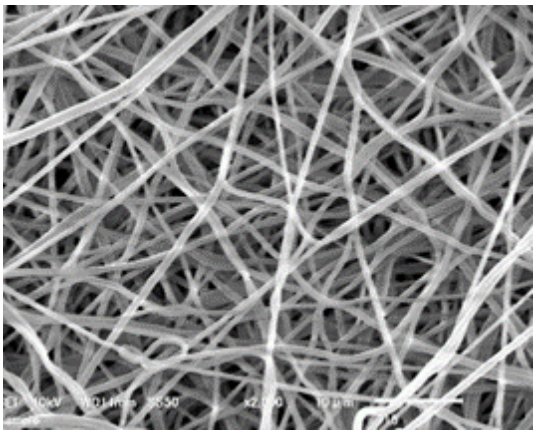

(c)

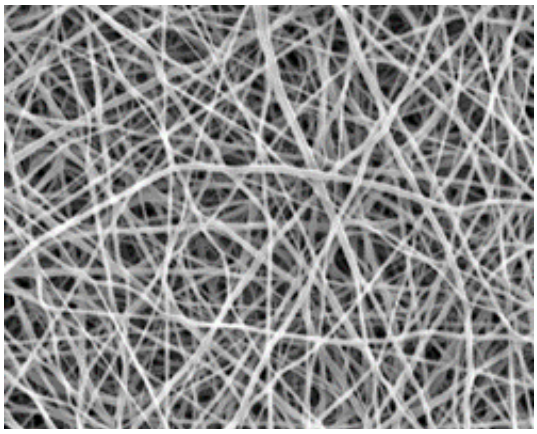

(d)

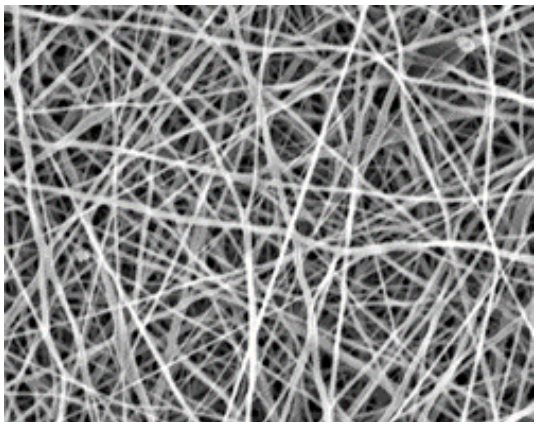

(e)

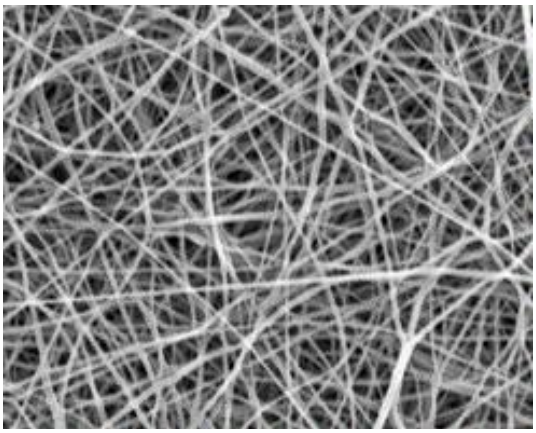

(f)

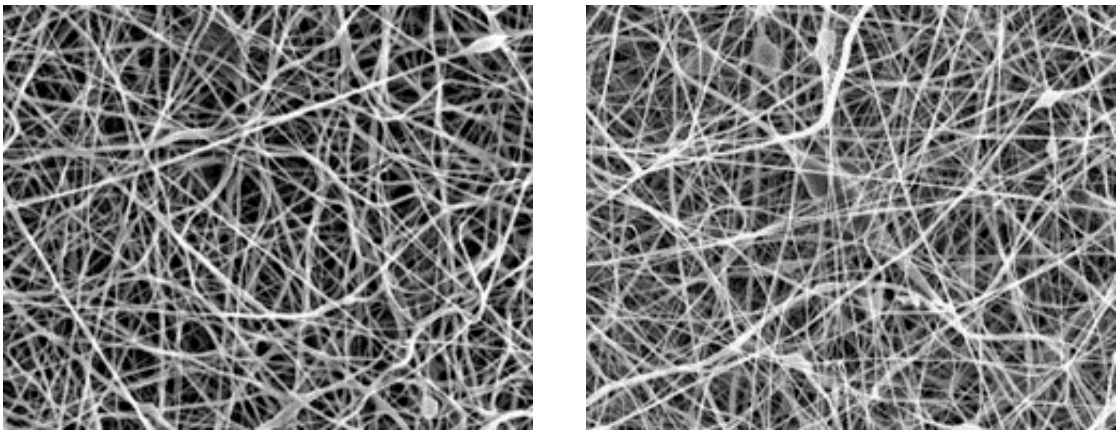

(g) (h)

Fig. 11. SEM images of block type PUSX nanofibers. (a)PU, (b)Si01, (c)Si02, (d)Si03, (e)Si04, (f)Si01-20, (g)Si01-40, (h)Si01-59 under optimized conditions. (Magnification: 2000, DMF/MEK=64:36)

Table 3. Average diameters of block type PUSX nanofibers under optimized spinning conditions.

Sample	*Polymer Concentration (wt%)*	*Voltage (kV)*	*Average Diameter(nm)*	*SD (nm)*
PU	15	20	720	215
Si01	20	20	636	179
Si02	20	20	690	150
Si03	15	20	548	128
Si04	13	20	440	89
Si01-20	13	17	531	142
Si01-40	10	17	402	94
Si01-59	10	17	471	111

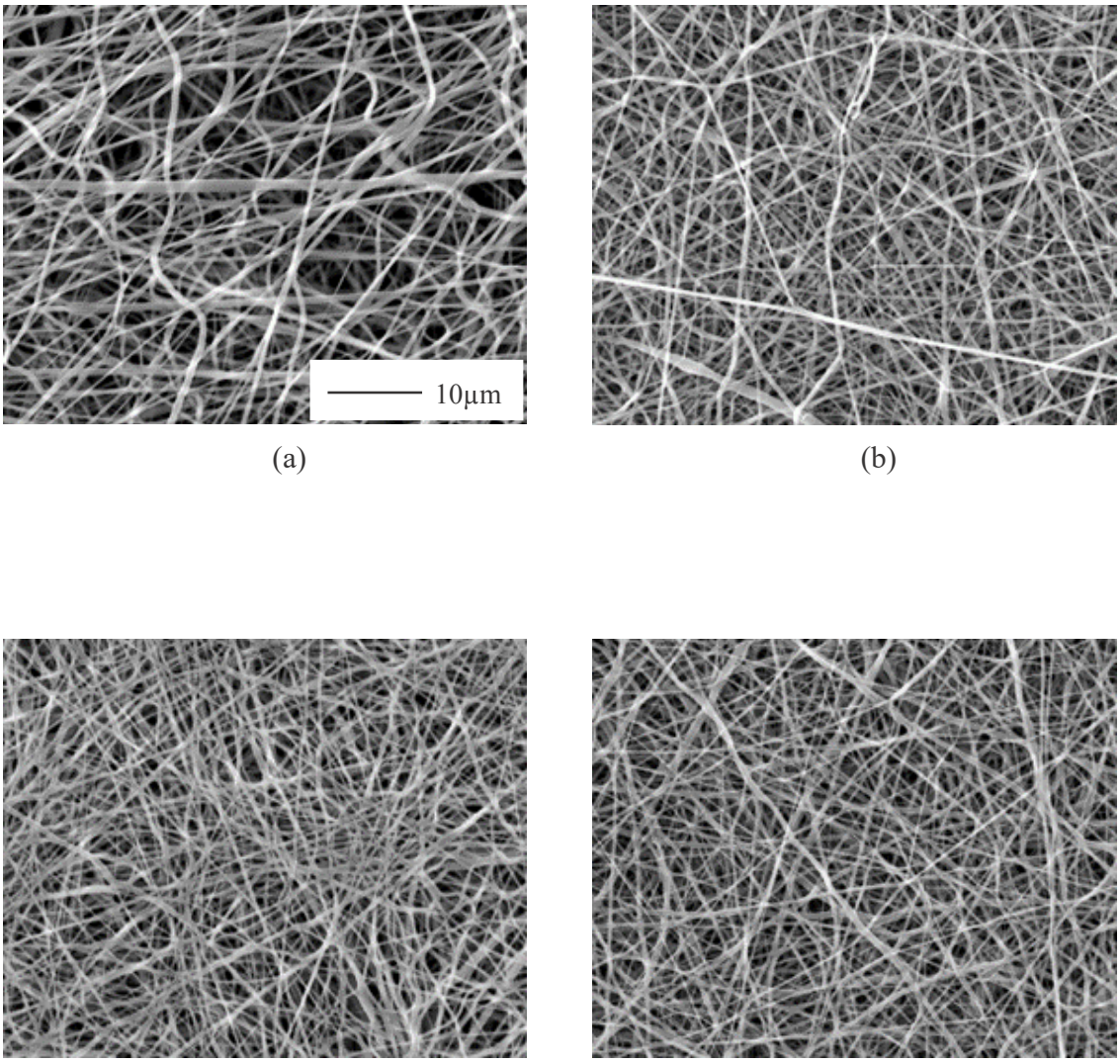

Fig. 12. SEM images of graft type PUSX nanofibers. (a) Si05, (b) Si06, (c) Si07, (d) Si08 under optimized conditions. (Magnification: 2000, DMF/MEK=64:36)

Table 4. Diameters of graft type PUSX nanofibers under optimized spinning conditions.

Sample	*Concentration (wt%)*	*Voltage (kV)*	*Average Diameter (nm)*	*SD (nm)*
Si05	15	15	564	142
Si06	15	15	544	124
Si07	15	15	456	117
Si08	15	15	456	129

3.8 Conclusion

In this chapter, we successfully prepared 12 kinds of PUSX nanofibers under the optimized conditions and investigated the effects of solvents, solution concentrations and temperature on the electrospinnability of PUSX solutions. This is the first time we suggest a way of preparing PUSX nanofibers during past decades instead of making silicone and PU into composite and then preparing into nanofibers or films. We reported a new material which has the advantages of both PU nanofiber and silicone. Silicone groups can have more effects on block type PUSX than graft type. The optimal polymer concentration for electrospinning and the average diameters of the obtained nanofibers decreased with the increase of both silicone chain length and silicone concentration in block type PUSX nanofibers as well as the decrease of viscosity and surface tension. Graft type PUSX nanofibers could not show clear influence of silicone chain length on electrospinning parameters.

3.9 References

[1] K. Yoon, B. S. Hsiao and B. Chu, J. Mater. Chem., 2008, 18, 5326– 5334.

[2] I. Siro and D. Plackett, Cellulose, 2010, 17, 459–494.

[3] H. Takagi and A. Asano, Composites: Part A, 2008, 39, 685–689.

[4] Wenguo Cui, et al. Investigation on process parameters of electrospinning system through orthogonal experimental design, Journal of Applied Polymer Science, Volume103, Issue5, pp 3105-3112, 2007.

[5] Zheng Ming Huang, et al. A review on polymer nanofibers by electrospinning and their applications in nanocomposites, Composites Science and Technology, 63, pp 2223–2253, 2003.

[6] Haitao Zhuo, et al. Preparation of polyurethane nanofibers by electrospinning, Applied Polymer Science, Volume109, Issue 1, pp 406-411, 2008.

[7] F. Cengiz, et al. The effect of salt on the roller electrospinning of polyurethane nanofibers, Fibers and Polymers, Volume 10, Issue 2, pp 177-184, 2009.

[8] S. Thandavamoorthy, et al. Self-assembled honeycomb polyurethane nanofibers, Applied Polymer Science, Volume101, Issue5, pp 3121-3124, 2006.

[9] Haitao Niu, et al. Ultrafine PDMS fibers: preparation from in situ curing-electrospinning and mechanical characterization, RSC Advances, 4(23):11782, 2014.

[10] Ruiping Xue, et al. Polydimethylsiloxane Core-Polycaprolactone Shell Nanofibers as Biocompatible, Real-Time Oxygen Sensors, Sens Actuators B Chem, 192: 697-707, 2014.

[11] Miriam Haerst, et al. Silicone Fiber Electrospinning for Medical Applications, 6th European Conference of the International Federation for Medical and Biological

Engineering, pp 537-540, 2014.

[12] Aneta, C.; Randal, H.; Randall, S.; Steven, S.; Dow Corning Corporation. Article comprising fibers and a method of forming the same. WO/2009/067232. 28 May 28 2009.

[13] Kazuko, S.; Toshimi, F.; Hitomi, M. Polysilsesquioxane-based nonwoven cloth and method of producing the same, separator for battery, and lithium secondary battery. JP-A 2014-025157. 6 February 6 2014.

[14] T. Ondarcuhu, C. Joachim. Drawing a single nanofibre over hundreds of microns. Europhys Lett., 42 (2) (1998), pp. 215-220.

[15] C.R. Martin. Membrane-based synthesis of nanomaterials. Chem. Mater., 8 (1996), pp. 1739-1746.

[16] P.X. Ma, R. Zhang. Synthetic nano-scale fibrous extracellular matrix. J Biomed Mat Res., 46 (1999), pp. 60-72.

[17] G.J. Liu, J.F. Ding, L.J. Qiao, A. Guo, B.P. Dymov, J.T. Gleeson, et al. Polystyrene-block-poly (2-cinnamoylethyl methacrylate) nanofibers-Preparation, characterization, and liquid crystalline properties. Chem.-A European J., 5 (1999), pp. 2740-2749.

[18] H. Fong, D.H. Reneker. Electrospinning and formation of nanofibers. D.R. Salem (Ed.), Structure formation in polymeric fibers, Hanser, Munich (2001), pp. 225-246.

[19] Zheng-Ming Huang, et al. A review on polymer nanofibers by electrospinning and their applications in nanocomposites. Composites Science and Technology. Volume 63, Issue 15, November 2003, Pages 2223-2253.

[20] R. Kessick, J. Fenn, G. Tepper. Polymer2004,45, 2981.

[21] G.I. Taylor. (3rd Ed.), Proc. Roy. Soc. London, A313 (1969), p. 453

[22] Jayesh Doshi, Darrell H.Reneker. Electrospinning process and applications of electrospun fibers. Journal of Electrostatics. Volume 35, Issues 2–3, August 1995, Pages 151-160.

[23] a) D. H. Reneker, I. Chun,Nanotechnology1996,7, 216. b) A. Fre-not, I. S. Chronakis,Curr. Opin. Colloid Interface Sci.2003,8, 64.c) Z.-M. Huang, Y.-Z. Zhang, M. Kotaki, S. Ramakrishna,Compos.Sci. Technol.2003,63, 2223

[24] Dan Li, Younan Xia. Electrospinning of Nanofibers: Reinventing the Wheel? Adv. Mater.2004, 16, No. 14, July 19.

[25] Toki Sangyo Co., Ltd. TVB-10M, www.tokisangyo.co.jp/product/keiki/TVB10.html

[26] www.face-kyowa.co.jp/products/3-3_SurfaceTension/dy500.html

[27] T. A. Nirmal Peiris. Microwave-assisted processing of solid materials for sustainable energy related electronic and optoelectronic applications.

[28] Adnan Haider, et al. A comprehensive review summarizing the effect of electrospinning parameters and potential applications of nanofibers in biomedical and biotechnology. Arabian Journal of Chemistry, Volume 11, Issue 8, December 2018, Pages 1165-1188.

[29] S. Haider, Y. Al-Zeghayer, F. Ahmed Ali, A. Haider, A. Mahmood, W. Al-Masry, M. Imran, M. Aijaz. Highly aligned narrow diameter chitosan electrospun nanofibers. J. Polym. Res., 20 (4) (2013), pp. 1-11

[30] Z. Shamim, B. Saeed, T. Amir, R. Abo Saied, Damerchely Rogheih. The effect of flow rate on morphology and deposition area of electrospun nylon 6 nanofiber. J. Eng. Fabrics Fibers, 7 (4) (2012), p. 42

[31] J. Lannutti, D. Reneker, T. Ma, D. Tomasko, D. Farson. Electrospinning for tissue

engineering scaffolds. Mater. Sci. Eng., C, 27 (3) (2007), pp. 504-509.

[32] H. Fong, I. Chun, D.H. Reneker. Beaded nanofibers formed during electrospinning. Polymer, 40 (16) (1999), pp. 4585-4592.

[33] S. Megelski, J.S. Stephens, D. Bruce Chase, J.F. Rabolt. Micro- and nanostructured surface morphology on electrospun polymer fibers. Macromolecules, 35 (22) (2002), pp. 8456-8466.

[34] Zhong X H, et al. Structure and process relationship of electrospun bioabsorbable nanofiber membranes. Polymer 43 pp. 4403, 2002.

[35] Siqi Huan, et al. Effect of Experimental Parameters on Morphological, Mechanical and Hydrophobic Properties of Electrospun Polystyrene Fibers, Materials (Basel). 8(5), 2718-2734, 2015.

[36] Guang-Zhi Yang, et al. Influence of Working Temperature on The Formation of Electrospun Polymer Nanofibers. Nanoscale Res Lett. 2017; 12: 55.

[37] Oliver Hardick, et al. Nanofibre fabrication in a temperature and humidity controlled environment for improved fibre consistency, Journal of Materials Science, Volume 46, Issue 11, pp 3890–3898, 2011.

[38] Ji Zhou, et al.Temperature Effect on the Mechanical Properties of Electrospun PU Nanofibers.Nanoscale Res Lett. 2018; 13: 384.

Chapter 4

Reproducibility and upscaling

4 Reproducibility and upscaling

4.1 Introduction

One of the greatest drawbacks of electrospinning is relatively low rate of generating large mass or volume of nanofibers. Though the benefits of electrospinning technologies have been largely demonstrated for many application fields where polymer nanofibers can be used, there is still a strong need to implement the production in the most efficient way, in order to address the pressing issues concerning: (i) large volume processing, (ii) accuracy and reproducibility in all the fabrication stages, and (iii) safety and environmental attributes of electrospinning. The scaling capability of the process and the technological issues explored to date evidence that free-surface methods exhibit high up-scaling potentialities in terms of production volumes. Productivity enhancement on a comparable industrial scale to that of conventional polymeric fibers is currently under active investigation, with emphasis on multi-jet electrospinning.[1-3] Multi jet technology is critical as a means of increasing the throughput of the electrospinning process and a detailed investigation is particularly significant. Although multi jet electrospinning is much more complicated than the single jet process, it has been demonstrated to be an optimal approach for enhancing electrospinning productivity rather than substantially increasing the throughput of a single spinneret.[4] Recently, modified single needle, multi needle and needleless systems have been introduced to achieve multiple polymer jets and thus improve the output of nanofibers. In this chapter, we mainly discussed about the upscaling of PUSX nanofibers by multi jet method.

4.2 Experimental section

To verify the reproducibility of the process, a pilot scale vertical electrospinning set-up (Nafias ES300, NafiaS Inc, Japan, as shown in Fig. 13) was utilized. 5 tips of plastic injection needles (ø0.70mm, length 38mm) were used and placed vertical to the floor. The collector was settled above the tips. The humidity was 50%RH and spinning temperature was 22℃ under the control of a small-sized air compressor (HITACHI PO-0.75 PG6) and micro flow rate temperature and humidity control apparatus (Kotohira KTC-Z15A).

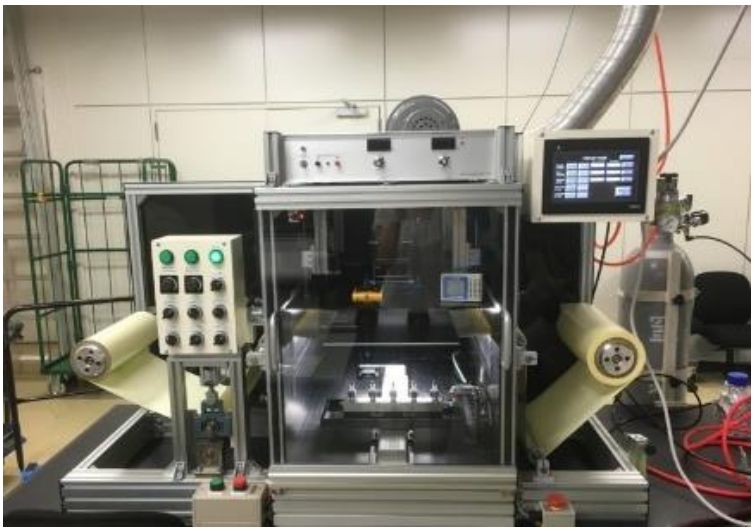

(a)

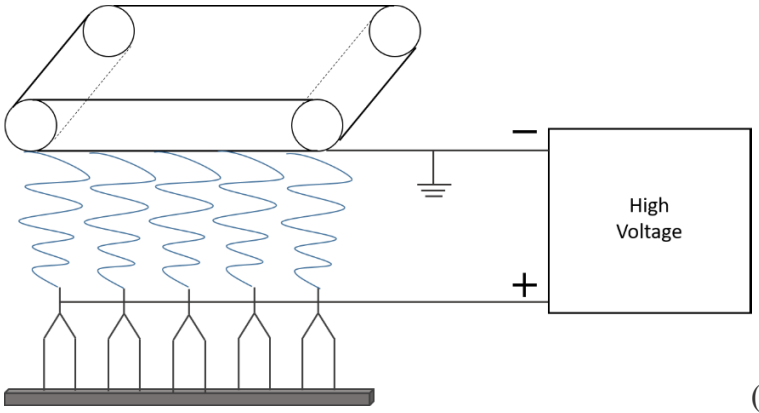

(b)

Fig. 13. (a)The pilot scale electrospinning set-up and the schematic illustration of multi jet electrospinning set-up.

4.3 Results and discussions

Many advanced applications and active polymer materials are still limited due to the lack of reliable and affordable electrospinning approaches which can guarantee the very high needed accuracy and reproducibility of the fabrication process, and the convergence between theoretical modeling and real-time control over the involved parameters which would be useful in this respect to offer new processing solutions extending the variety of usable compounds.[5] Finally, it is largely demonstrated that ambient conditions strongly influence the properties of electrified jets and of resulting electrospun materials, and even small environmental perturbations can cause significant variations of the fiber properties. To address this issue, many providers of commercial set-ups have developed proprietary climate-controlled electrospinning systems guaranteeing temperature and humidity control within certain ranges.

Another important concern regards process environmental issues about solvent electrospun materials. This aspect is very important not only for safety reasons during processing, but also for final products since solvent residues could be trapped inside the produced nanofibers. Solvent-based electrospinning with high control over fiber morphology and functionality could be safely used in nontextile applications where production volumes are moderate (e.g., nanoelectronics), whereas an accurate control over solvent residuals become crucial for biomedical and pharmaceutical applications.

To investigate the reproducibility of the optimized electrospinning processes using the lab scale set-up and to verify if the optimized conditions can be readily transferred to other devices, the electrospinning process was repeated on a pilot scale device. The combination of a number of individual needles as the spinneret of electrospinning setups is the most

direct method to increase nanofiber production. The processing parameters and various polymer solution concentrations for PUSX Si01 applied on pilot scale electrospinning device are presented in Table 5, the possibility of upscale electrospinning under varying nozzle diameters were discussed.

In Table 5, SEM images of the electrospun fibers illustrate the good quality (uniform, continuous and beadless fibers). In addition, the average diameter is also plotted in Table 6 as well as the optimal parameters for upscaling. For the purpose of commercializing nanofibrous membranes high-volume production is essential, especially for industrial development in biomedical applications such as tissue engineering, wound dressings, drug delivery and for air/liquid filtration and textile applications as well.[5] Considering the growing interest in PUSX for high performance applications, the ability to process PUSX nanofibers in larger quantities was evaluated by a pilot scale set-up, operated with 5 needles in parallel, and a conveyer belt allowing coating of large areas by continuous electrospinning. Table 5 also shows that the diameter and quality of PUSX fibers obtained by the lab and pilot scale devices are very similar and controllable. To investigate the reproducibility and to verify the previously optimized parameters, we tried the 20wt% solution and 19G nozzle needle (ø0.6mm) at first. It turned out that the diameter was not as small as we performed on the lab scale set-up. As we know, decreasing nozzle diameter has the effect of decreasing fiber diameter, distribution and productivity.[6] In order to obtain finer fibers, smaller nozzle needles, such as 21G (ø0.5mm) and 22G (ø0.4mm) were also used to investigate the most suitable parameters on the pilot scale set-up. However, 20wt% solution was too viscous to form a smooth and stable flow so that lower concentration became essential. And the different fiber dimension was influenced by both the

concentration and the nozzle diameter.

This experiment demonstrates the feasibility of upscaling the PUSX nanofibers electrospinning process. By controlling the swing speed, rolling speed and other parameters, we are able to get nanofibrous sheet with various and controllable thickness and area. Worth mentioning that we had successfully prepared nanofibers on this pilot scale setup for more than 72h and obtained nanofiber sheets with an area larger than 23×290cm and thickness of 0.155-0.175mm.

Table 5. The processing parameters and optimal parameters of PUSX Si01 nanofibers on pilot scale device (Magnification: 2000)

	PUSX Si01 nanofiber			
Solvent	DMF:MEK = 64:36			
Voltage (kV)	15			
Nozzle type	19G(0.6mm)	21G(0.5mm)	22G(0.4mm)	22G(0.4mm)
Solution concentration (wt%)	20	15	15	12.5
SEM image	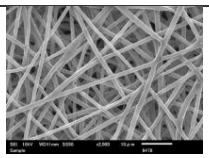	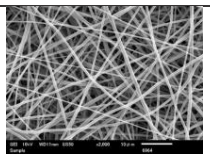	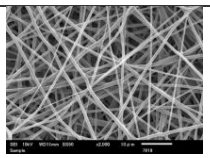	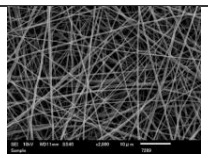
Average diameter (nm)	1260	548	524	310
SD (nm)	220	167	137	102
Optimal parameters	Solvent: DMF:MEK = 64:36 Voltage: 15~15.5kV Nozzle type: 22G(0.4mm) Solution concentration: 15wt% Distance: 10cm Flow rate: 0.1mL/min Humidity: 50%RH Temperature: 18~25℃ Swing speed: 40mm/sec Rolling speed: 1mm/min			

4.4 References

[1] Yuris Dzenis. Spinning Continuous Fibers for Nanotechnology, Science, Vol 304, Issue 5679, 2004.

[2] Christian Burger, et al. Nanofibrous materials and their applications, Annual Review

of Materials Research, Volume 36, pp 333-368, 2006.

[3] Andreas Greiner, et al. Electrospinning: A Fascinating Method for the Preparation of Ultrathin Fibers, Angewandte Chemie, Volume46, Issue30, pp 5670-5703, 2007.

[4] Feng-Lei Zhou, et al. Mass production of nanofiber assemblies by electrostatic spinning, Polym Int 2009; 58: pp 331-342, 2009.

[5] L. Persano, et al. Industrial upscaling of electrospinning and applications of polymer nanofibers: a review, Macromol, Mater. Eng., 298 (5), pp 504-520, 2013.

[6] Heikkila P, et al. Parameter study of electrospinning of polyamide-6, European Polymer Journal, Volume 44, Issue 10, pp 3067-3079, 2008.

Chapter 5

Characterization

5 Characterization

5.1 Introduction of Fourier transform infrared spectroscopy (FTIR)

As the systems were superseded by the much more powerful FT-IR (Fourier-Transform-Infrared) spectrometers, IR spectroscopy progressed into a widely used analytical tool. An advantage of FT-IR spectroscopy is its capability to identify functional groups such as C=O, C-H or N-H. Most substances show a characteristic spectrum that can be directly recognized. In this research, attenuated total reflectance-Fourier transform infrared spectroscopy (ATR-FTIR) was selected to analyze the chemical structures of the materials. The technique of Attenuated Total Reflectance (ATR) has in recent years revolutionized solid and liquid sample analyses because it combats the most challenging aspects of infrared analyses, namely sample preparation and spectral reproducibility. ATR is ideal for strongly absorbing or thick samples which often produce intense peaks when measured by transmission. ATR works well for these samples because the intensity of the evanescent waves decays exponentially with distance from the surface of the ATR crystal, making the technique generally insensitive to sample thickness. Other solids that are a good fit for ATR include homogeneous solid samples, the surface layer of a multi-layered solid or the coating on a solid. Even irregular-shaped, hard solids can be analyzed using a hard ATR crystal material such as diamond. Ideal solids include: Laminates, paints, plastics, rubbers, coatings, natural powders and solids that can be ground into powder. The advantages of ATR are as follows: (1) Minimal sample preparation—place the sample on the crystal and collect data, (2) Fast and easy cleanup—simply remove the sample and clean the surface of the crystal, (3) Analysis of samples in their natural states—no need to heat, press into pellets, or grind in order to collect spectra, and (4) Excellent for thick or strongly absorbing

samples—ideal for difficult samples like black rubber. As mentioned, the major benefit of ATR is the ability to measure a wide variety of solid and liquid samples without requiring complex preparations. The basic principle is described in Fig. 14. The ATR crystal comprises an IR transparent material with a high refractive index and polished surfaces as shown in Fig. 14a.[1] The infrared beam enters the ATR crystal at an angle of typically 45° (relative to the crystal surface) and is totally reflected at the crystal to sample interface. Because of its wave-like properties, the light is not reflected directly by the boundary surface but by a virtual layer within the optically less dense sample (as shown in Fig. 14b). The fraction of light reaching into the sample is known as evanescent wave. Its penetration depth depends on the wavelength, the refractive indices of the ATR crystal and the sample and the angle of the entering light beam. It is typically of the order of a few microns (0.5-3 μm). In the spectral regions where the sample absorbs energy, the evanescent wave is attenuated. After one or several internal reflections, the IR beam exits the ATR crystal and is directed to the IR-detector.

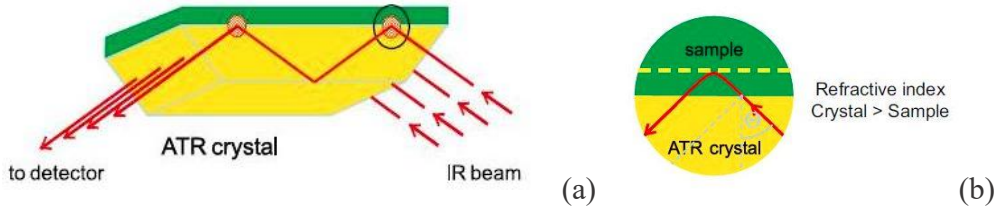

Fig. 14 (a) Schematic illustration of ATR principle and (b) ATR effect.[1]

5.2 Experiment and results

In this chapter, Attenuated total reflectance-Fourier transform infrared spectroscopy (ATR-FTIR, IR Prestige-21, Shimadzu Corporation, Japan, as shown in Fig. 15) was

carried out to analyze the chemical structure of PUSX nanofibers. All spectra were taken in an absorption mode between the wavenumber range of 4000–700 cm^{-1} with resolution of 4cm^{-1} and accumulation of 20 scans. The number of specimens observed for each polymer was 3.

Fig. 15. Attenuated total reflectance-Fourier transform infrared spectroscopy.

Fourier transform infrared spectroscopy (FTIR) by using ATR for different kinds of PUSX nanofibers was used to observe the chemical structural differences due to the incorporation of silicone group to the PU polymer chain and electrospinning process. Fig. 16 shows the characteristic infrared spectra of the samples.

From Fig. 16 we can find that the absorption occurs around 3420-3200cm^{-1} (NH stretching), 3000-2800cm^{-1} (CH_2, CH_3 stretching), 1700cm^{-1} (urethane bond), 1510cm^{-1} (amideII bond) due to the structure of urethane. Also the peaks at 1250cm^{-1} (the bending of CH in Si-CH_3), 1100-1000cm^{-1} (Si-O-C stretching), 800cm^{-1} (Si-C stretching) are characteristic for silicone. The chemical structures of both urethane and silicone in PUSX can be observed from this spectra which shows that PU was successfully modified by

silicone groups. Especially in Fig. 14 (c), the peaks at 1100-1000cm^{-1} (Si-O-Si stretching), 800cm^{-1} (Si-C stretching) are strengthened with the increasing of silicone concentration in block type PUSX. Moreover, in spectra of PUSX Si01-59, peaks appeared at 3400-3200cm^{-1}, 3000-2800cm^{-1}, 1700cm^{-1} and 1510cm^{-1} (characteristic bands of urethane) were weakened because of the higher concentration of silicone. In Fig. 16(b) and (d), we can see that the peaks are very similar to each other in block type PUSX with different chain length and graft type PUSX. This shows that, the ratio of PU to silicone in the main chain has the most significant influence on chemical properties.

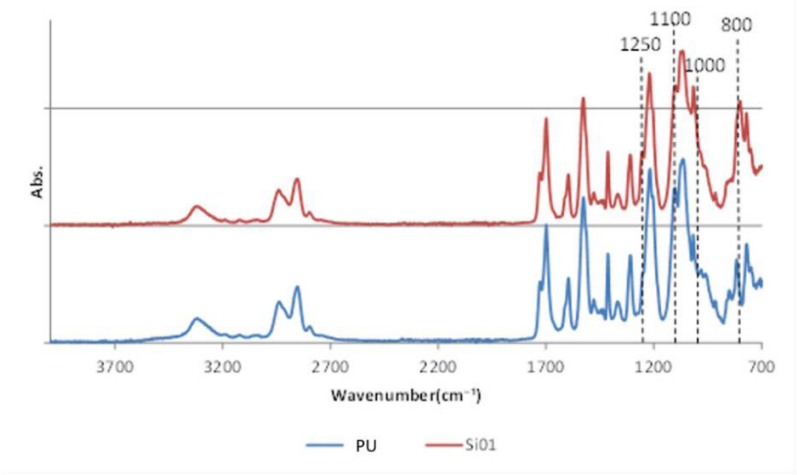

(a)

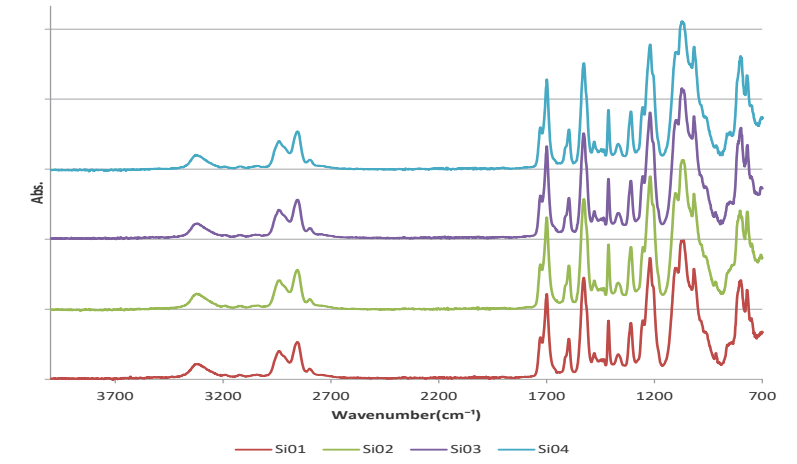

(b)

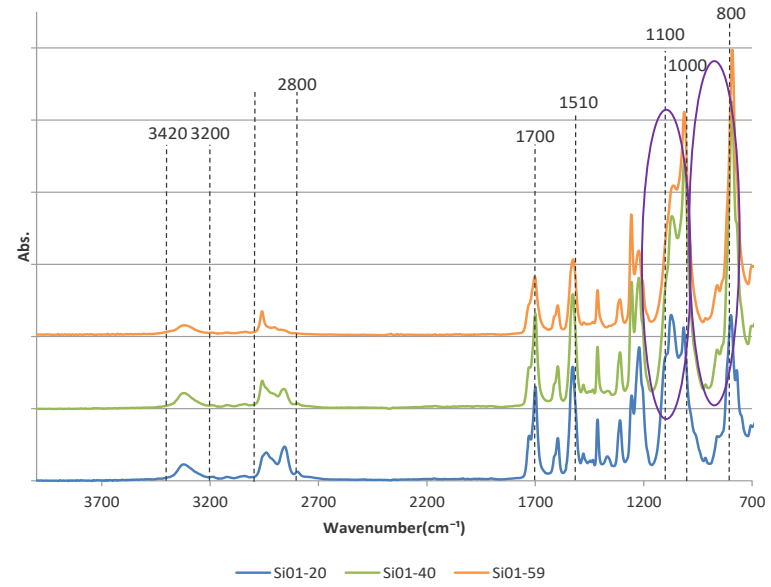

(c)

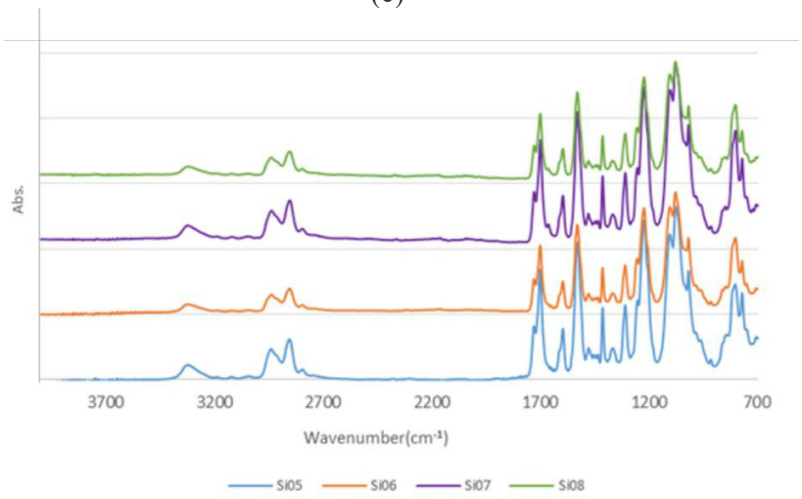

(d)

Fig. 16. FTIR spectra of PU and PUSX Si01 nanofibers (a), block type PUSX nanofibers with various chain length (b), block type PUSX nanofibers with various silicone concentration (c), graft type PUSX nanofibers with various chain length (d).

5.3 References

[1] Bruker Optics Inc. Attenuated Total Reflection (ATR)- a versatile tool for FT-IR spectroscopy, 2011.

Chapter 6

Physical properties

6 Physical properties

6.1 Introduction

Electrospun nanofibers have been used in various fields such as filtration, catalysis, clothing and biomedical applications because of the submicron size and high surface area along with the porous architecture.[1,2] Especially for biomedical applications, electrospun mats provide the lightness in weight, porosity, flexibility in technique, as well as the support for cell attachment and growth along with the exchange of nutrients and gases, which make them suitable for tissue engineering, wound dressing, drug delivery, health care, etc.[3] A non-woven matrix composed of nanofibers is easily produced via electrospinning, and is architecturally similar to the nanofibrous structure of extracellular matrix.[4] If necessary, the nanofibers can be further functionalized via incorporation with bioactive species (e.g. enzymes, DNAs, and growth factors) to better control the proliferation and differentiation of cells seeded on the scaffolds.[5] These attributes make electrospun nanofibers well-suited as scaffolds for tissue engineering.

Among various kinds of nanofibers, polyurethane nanofibers were selected as one of the most suitable choices for biomedical applications thanks to the unique properties of polyurethane. Electrospun polyurethane nanofibers have been successfully used in wound dressing thanks to an excellent oxygen permeability and barrier properties.[6] Water permeability is also important as it keeps the wound moist and prevents accumulation of fluid around the wound and on its cover. These covers perform a preventive function against infection with microorganisms, absorb blood and wound fluids to contribute to the healing process, and in some cases, to apply medical treatment to the wound.[7, 8, 9] However, there are still several limitations and disadvantages of polyurethane nanofibers to be

applied in biomedical field, such as poor thermal capability, poor weatherability and flammability. In order to improve the properties of polyurethane nanofibers, we tried to introduce silicone group into polyurethane polymer chains to fabricate silicone modified polyurethane (PUSX) and optimized the electrospinning parameters. In chapter 6 and 7, PUSX nanofibers were evaluated by physical properties and cell culture study and compared with films. The advantages of polyurethane, silicone and nanofibers are very attracted to this work. We expect this new material to be applied in many fields as an improved alternative of polyurethane nanofibers, such as wound dressing, tissue engineering because of the biocompatibility of silicone. Before going for the in vitro cell attachment and proliferation applications, the all prepared nanofibers are analyzed in detail by various methods and compared with films. To investigate the effect of different structure (block and graft type), chain length and silicone concentration, physical properties evaluation was performed. Tensile tests were performed to investigate the mechanical properties such as tensile strength, elongation at break and Young's modulus. The water contact angle (WCA) measurement and water retention tests were carried out to determine the hydrophobicity of PUSX material. Thermal conductivity was analyzed in order to discuss the heat retention ability of PUSX nanofibers and films.

6.2 Materials

All the electrospinning solutions were prepared by diluting the PUSX solutions (30 wt%) in DMF/MEK mixed solvent (v/v = 64:36) and stirring at room temperature for 48 hours in order to obtain homogeneous solutions. All electrospinning experiments were performed at room temperature (22℃) under the optimized parameters discussed in Chapter 3 and the

deposited nanofibers were collected on a moving metallic collector. A 10-20kV voltage was applied while needle tip to collector distance was 10 cm with the irradiation angle of 30º and air flow rate in spinning environment was 0.1mL/min.

Table 6. SEM morphologies and average diameter of PUSX nanofibers under the optimized electrospinning parameters (magnification: 2000)

Sample	PU	Si01	Si02	Si03
SEM	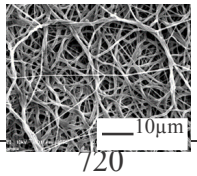	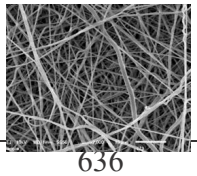	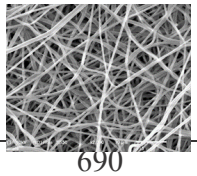	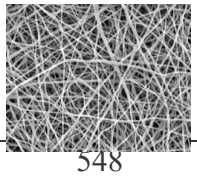
Average Diameter (nm)	720	636	690	548
Sample	Si04	Si01-20	Si01-40	Si01-59
SEM	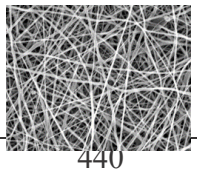	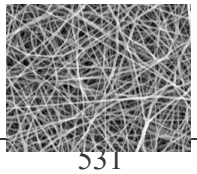	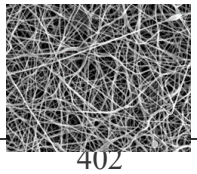	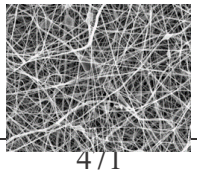
Average Diameter (nm)	440	531	402	471
Sample	Si05	Si06	Si07	Si08
SEM	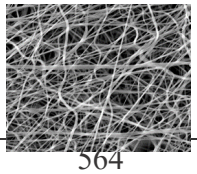	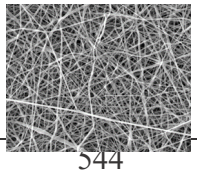	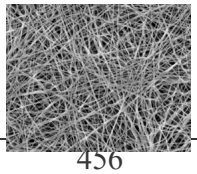	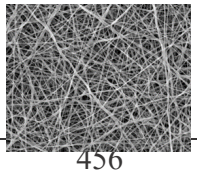
Average Diameter (nm)	564	544	456	456

6.3 Mechanical properties

Recent advances in nanotechnology have enabled materials and devices to be fabricated at the nanoscale. One of the motivations for the miniaturization process of materials is the superior mechanical properties that nano-sized materials possess as compared to bulk materials. Nanofibers in particular, have been used for a wide range of applications such as tissue engineering[10], filter media [11], reinforcement in composites[12] and micro/nano-

electro-mechanical systems (MEMS/NEMS). [13] During the service lifetime of the nanofibers, forces exerted on the fibers in the form of mechanical contact or thermal misfit may result in permanent deformation or even failure.[14] Therefore, there is a need to characterize the mechanical properties of nanofibers.

6.3.1 Experiments

Tensile testing is arguably the most common test method used in both force measurement and material testing. Tensile testing is used primarily to determine the mechanical behavior of a component, part or material under static, axial loading. The test method for both material testing and force measurement is similar; however the measurement results are different. A tensile test is performed to determine the tensile properties of a material or component. The test sample's deformation is used to characterize its ductility or brittleness as well as important characteristics such as tensile strength, yield point, elastic limit, percent elongation, elastic modulus and toughness.

In this research, tensile tests were performed by a compact table top universal tensile tester (EZTest/EZ-S, Shimadzu Corporation, Japan, as shown in Fig. 17a) for samples 10 mm long and 5 mm wide (as shown in Fig. 17b) at a crosshead speed of 10 mm/min. A test window frame is used to hold the nanofiber membrane and prevent unwanted stretching of the membrane prior to testing. The dimension of the test frame is shown in Fig. 17b. A smaller piece of the tab is used to sandwich the membrane in between. Epoxy glue may be used to secure the membrane to the tabs. A micrometer screw gauge may be used to determine the thickness of the membrane. However, since nanofibrous membrane is porous and generally soft, care must be taken to ensure that the membrane is not compressed

during measurement. If the membrane is found to be compressed, alternative method of thickness determination may be necessary. The test specimen(test window frame with the fiber) were mounted on the tensile tester such that the grip is on the tabs holding the fiber membrane following by cutting off a portion of the window frame as shown in the Fig. 17c. At least 10 specimens were tested for each sample. To compare the mechanical propertied of PUSX nanofibers with PUSX films, same tests were performed on PUSX films.

(a)

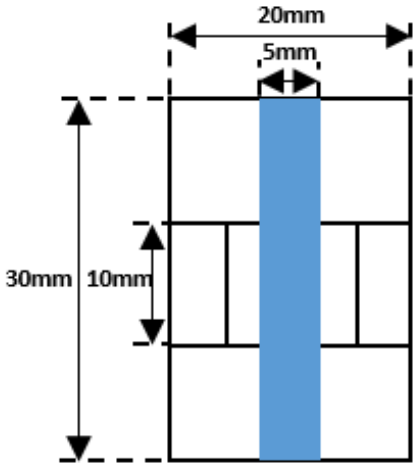

(b)

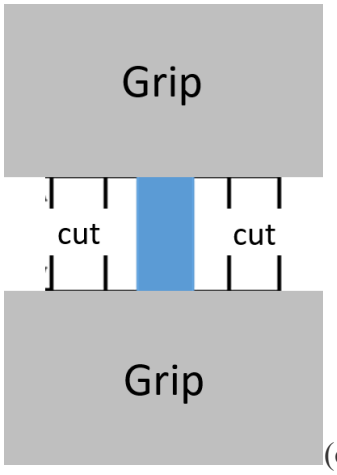

(c)

Fig. 17. (a) A compact table top universal tensile tester. (b) A paper template used to prepare tensile specimens of the electrospun non-woven fibrous mat. (c) Cutting of vertical ribs of frame prior to start of tensile test

Significance in physical properties were statistically analyzed by one-way analysis of variance (ANOVA) using R free software. Statistical significance was set at $p < 0.05$ to identify which group were significantly different from other groups.

6.3.2 Tensile strength

Fig. 18(a) (b) and (c) shows the graphs of the trend of tensile strength and comparison of all the samples. In all the 3 graphs, we may get a conclusion that PUSX films have better tensile strength than nanofibers because of the porosity and fiber orientation of nanofibers. Due to the porosity of nanofibers, the cross section area was apparent compared to the cross section area of films, which makes the tensile strength supposed to be higher than the results. Pure PU nanofibers show the highest strength because of the high mechanical properties of PU. From Fig.18 (a) and (b), we can see that for block type PUSX nanofibers, tensile strength increased with the increase of silicone chain length and Si04 samples with the longest silicone chain length (n=50) showed the highest tensile strength of 5.9MPa. Samples with longer silicone chain length showed smaller diameters and more improved orientation of the molecular chains while being prepared under the optimized parameters, which contributes to the higher tensile strength. Meanwhile, the tensile strength decreased with the increase of silicone concentration because of the low cohesive force of silicone structure and the decreasing concentration of PU. When the silicone concentration increases, the low cohesive force changed the tensile strength of the material. On the other hand, the increase of silicone concentration caused the decrease of the ratio of PU in the polymer and the weight percent of PU as well, which means the lack of the higher mechanical structure (PU). Tensile strength of films could not show much statistically

significance because of the random orientation of the molecular chains.

In the graph of graft type PUSX nanofibers and films (Fig. 18c), Si08 nanofiber showed the highest tensile strength of 6.8MPa with the Si05 sample showed the lowest result of 6.1MPa. There is almost no difference and trend to be observed because the results are in the same range. In this case, the silicone groups on the side chain are not able to influence the properties so much because the tensile strength is mainly determined by the high mechanical properties of PU in the main chain.

The tensile stress–strain curves of the electrospun PUSX nanofibers and PUSX films are shown in Fig. 18(d) and (e). Typical curves each from a different structure PUSX are plotted for an obvious comparison. From Fig. 18(d), we can clearly see the differences before and after the silicone modification. Si01-59 samples, with the highest silicone concentration in the block structure show the lowest mechanical performance of the fiber membrane because of the low cohesive force of silicone. Instead, the tensile stress–strain curves of PUSX films show very similar trend and much better mechanical performance because of the random orientation of the molecular chains.

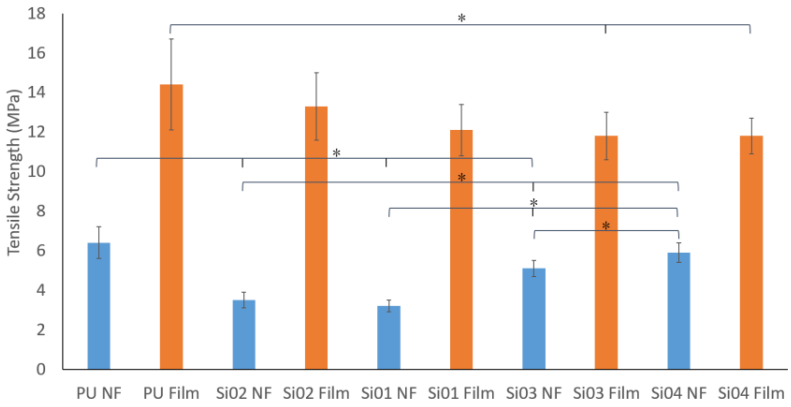

(a)

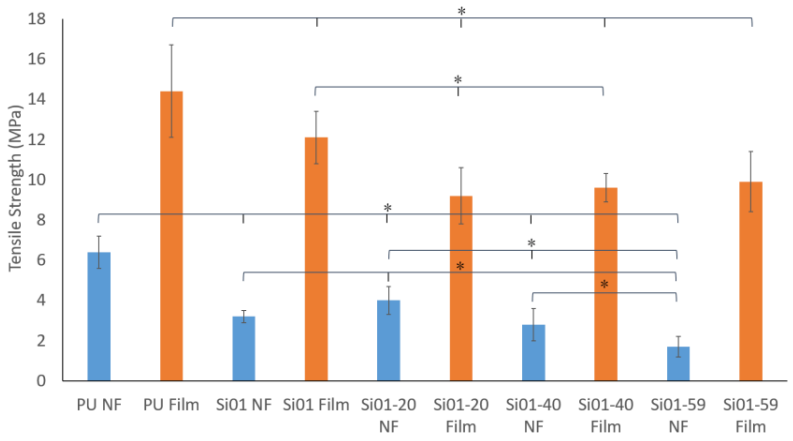
Tensile Strength (MPa)
18
16
14
12
10
8
6
4
2
0
PU NF
PU Film
Si01 NF
Si01 Film
Si01-20 NF
Si01-20 Film
Si01-40 NF
Si01-40 Film
Si01-59 NF
Si01-59 Film

(b)

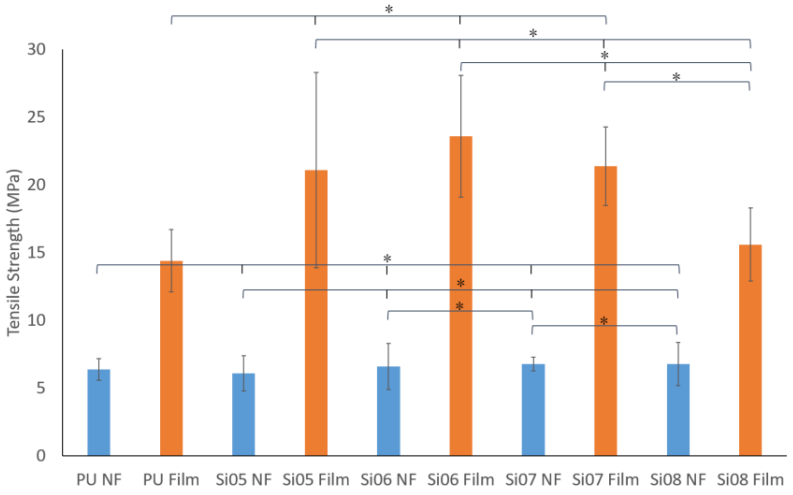
Tensile Strength (MPa)
30
25
20
15
10
5
0
PU NF
PU Film
Si05 NF
Si05 Film
Si06 NF
Si06 Film
Si07 NF
Si07 Film
Si08 NF
Si08 Film

(c)

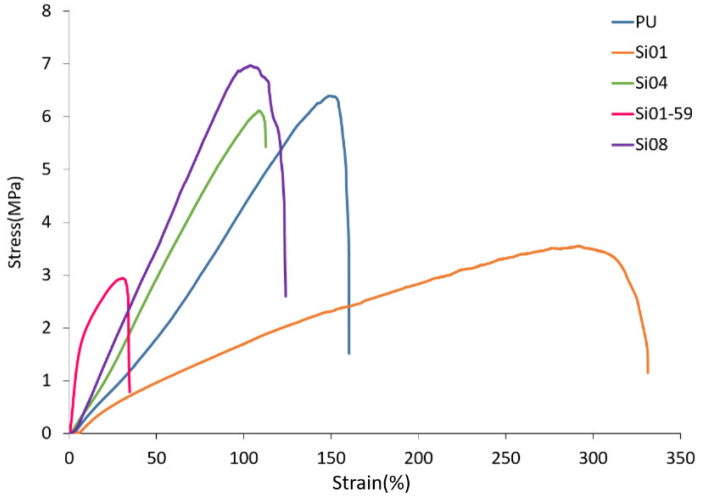
Stress(MPa)
8
7
6
5
4
3
2
1
0
0
50
100
150
200
250
300
350
Strain(%)
PU
Si01
Si04
Si01-59
Si08

(d)

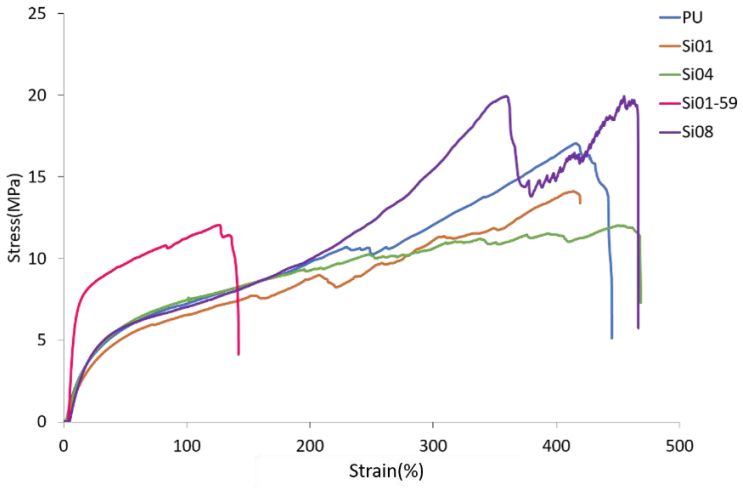

(e)

Fig. 18. Comparison of tensile strength (MPa) and stress-strain curve. "*" was statistically significant ($p < 0.05$) between each 2 samples. (a) Block type PUSX nanofibers and films with various chain length, (b) Block type PUSX nanofibers and films with various silicone concentration, (c) Graft type PUSX nanofibers and films with various chain length, (d) Stress-strain curve of PUSX nanofibers (e) Stress-strain curve of PUSX films.

6.3.3 Elongation at break

In Fig. 19, we can see that the elongation at break decreased with the increase of both silicone chain length and silicone concentration in block type PUSX nanofibers. For the PUSX nanofibers with different silicone chain length, the increase of silicone chain length caused the decrease in fiber diameters under optimized conditions, which lead to the increase of entanglement and frictional resistance in nanofibers. And for PUSX nanofibers with different silicone concentrations, the increase of silicone concentration means the decrease of polyurethane concentration in molecular chains, the high elongation property of polyurethane became difficult to be observed. Meanwhile, the elongation at break of graft type PUSX nanofibers show very similar results to each other for the same reason

with the tensile strength. As for graft type, the elongation at break does not show an obvious trend, the silicone groups on the side chains are not able to influence the properties because the ratio of polyurethane and silicone in the molecular chain cannot change with the increase of chain length. PUSX films have better tensile strength than nanofibers because of the porosity and fiber orientation of nanofibers.

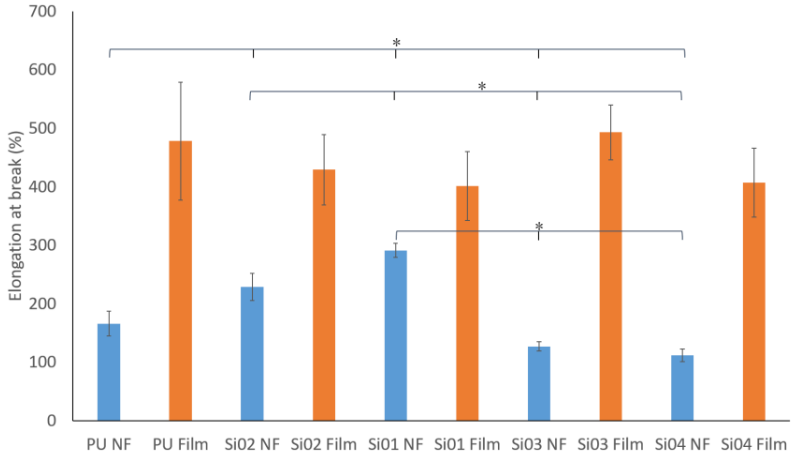

(a)

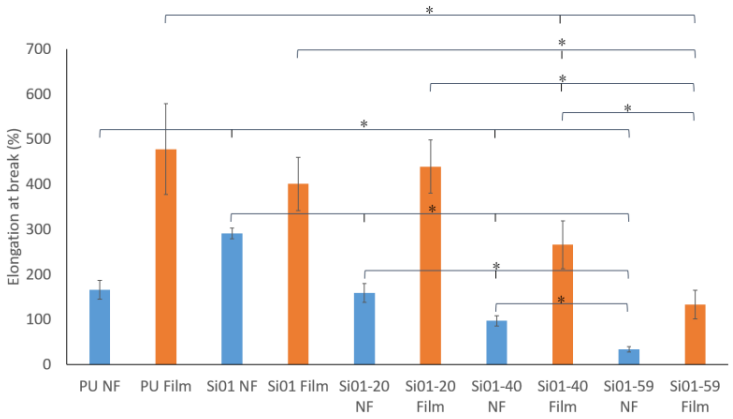

(b)

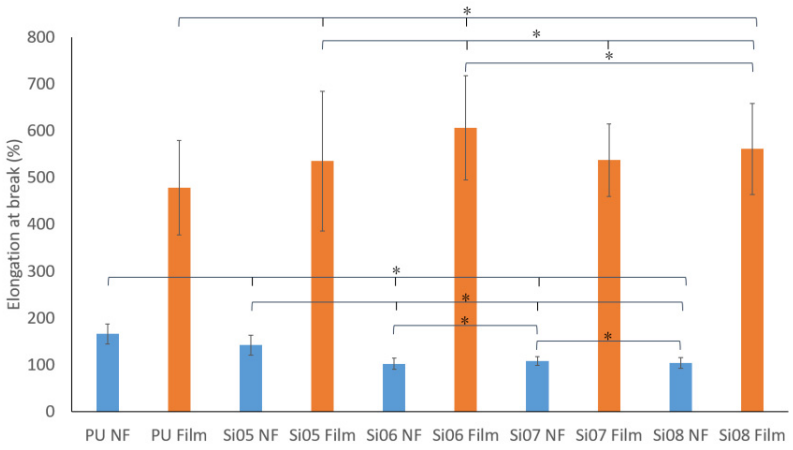

(c)

Fig. 19. Comparison of elongation at break (%). "*" was statistically significant ($p < 0.05$) between each 2 samples. (a) Block type PUSX nanofibers and films with various chain length, (b) Block type PUSX nanofibers and films with various silicone concentration, (c) Graft type PUSX nanofibers and films with various chain length.

6.3.4 Young's modulus

From Fig. 20, we can see that the Young's modulus increased with the increase of both chain length and silicone concentration in block type PUSX nanofibers. As silicone chain length and concentration increased, the concentration of PU became lower and lower, the characteristic of PU (high elongation at break) became difficult to observe, which means the samples are more elastic. Moreover, the existence of silicone also makes it more difficult to change the shape of the samples.

For both block and graft type PUSX nanofibers, all the tensile test results show that PUSX films have higher tensile strength than nanofibers. This phenomenon can be explained by the orientation of polymer chain and different structures of nanofibers and films (porosity and density).

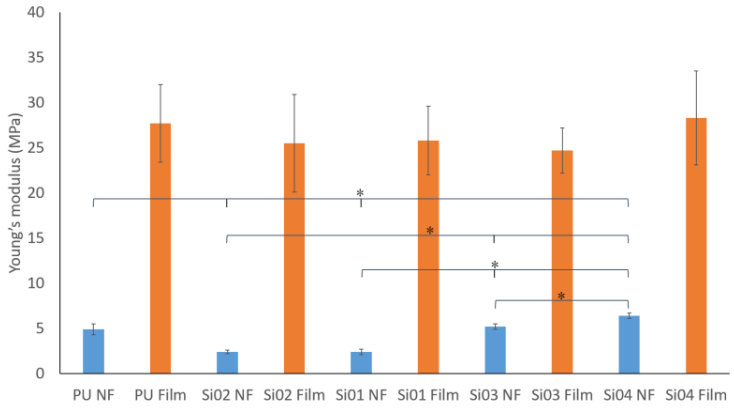

(a)

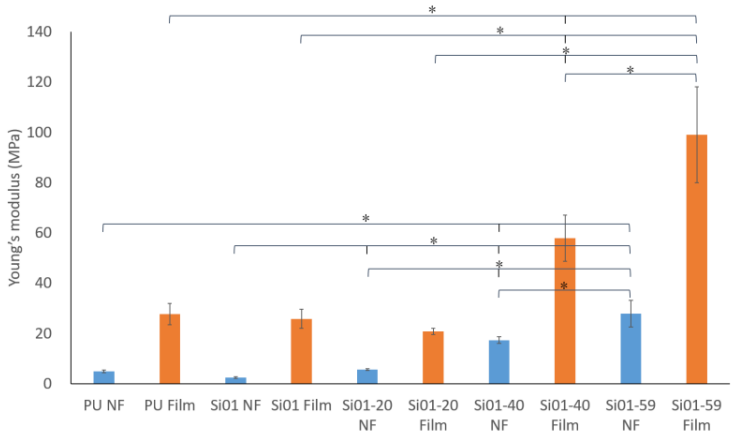

(b)

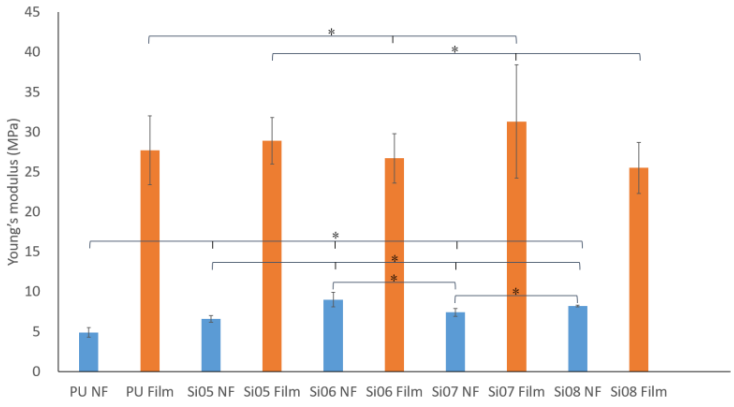

(c)

Fig. 20. Comparison of Young's modulus (MPa). "*" was statistically significant ($p < 0.05$) between each 2 samples. (a) Block type PUSX nanofibers and films with various chain length, (b) Block type PUSX nanofibers and films with various silicone concentration, (c) Graft type PUSX nanofibers and films with various chain length

6.3.5 Summary

Electrospinning has proven to be an efficient method to produce thin fibers with diameters down to the nano-scale. However, the mechanical properties of these nanofibers are often well below those of fibers made by conventional processes such as melt spinning or solution spinning or films made by casting process. The introduction of silicone groups into the polyurethane chain leads to the decrease of mechanical strength because of the lower cohesive force of silicone structure.

6.4 Thermal conductivity

6.4.1 Experiments

An ever increasing interest has been focused on heat and mass transfer processes in porous media due to their growing importance in functional material design, thermal managements of microsystems, and even in bio-medical engineering.[15-19] Among them the high-porosity foam materials have been discussed during the past years. The polymeric foams have been used as the efficient thermal insulation materials because of the poor thermal transport performance.[20-23] Especially for polyurethane foams, the thermal conductivity has been discussed by a lot of researchers because PU foam has been applied as pre-insulated district heating pipes for several decades. For instance, Tseng et al. investigated theoretically and experimentally the thermal conductivity of the polyurethane foam in the temperature range between 300 and 20 K for the development of liquid hydrogen storage tanks.[24] Jhy-Wen Wu et al. reported a theoretical and experimental study of the thermal performance of an evacuated polyurethane (PU) foam insulation system by 6 different cell sizes ranging from 150 to 350 μm of PU foam insulation.[22] However, as one

of the most unignorable porous structure material of PU, PU nanofibers, especially PUSX nanofibers were seldom discussed till now.

In our research, the thermal conductivities were determined by KES-F7 Thermal Labo IIB precision rapid thermal property measurement unit (Kato Tech Co., Ltd, Japan). The temperature of water box was set to room temperature. Then samples (5×5cm) were placed on water box and the heat plate of B. T. box was put on the upper surface of the samples. After reaching a constant value, the heat flow loss W (watt) of B.T. using panel meter was recorded. Steady heat flow lost is calculated as following equation:

$$W= K \cdot A \cdot \triangle T/D,$$

where D is the thickness of samples (cm), A is the area of B.T. heat plate (cm2), △T is the temperature difference of sample (℃), K is thermal Conductivity. Thermal conductivity K will be shown as following equation:

$$K= W \cdot D/A\triangle T \ (W/cm℃)=100 \ W \cdot D/A\triangle T(W/mK).$$

When measuring with the B. T. Box, the applied pressure could be adjusted variably. Standard value was set to be 6g/cm2. The temperature of the B. T. Box heat plate was controlled with an error of less than 0.1℃.

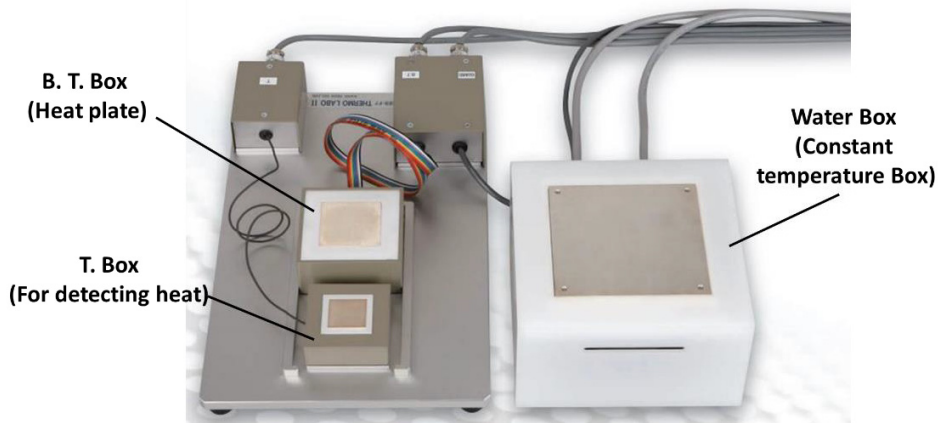

(a)

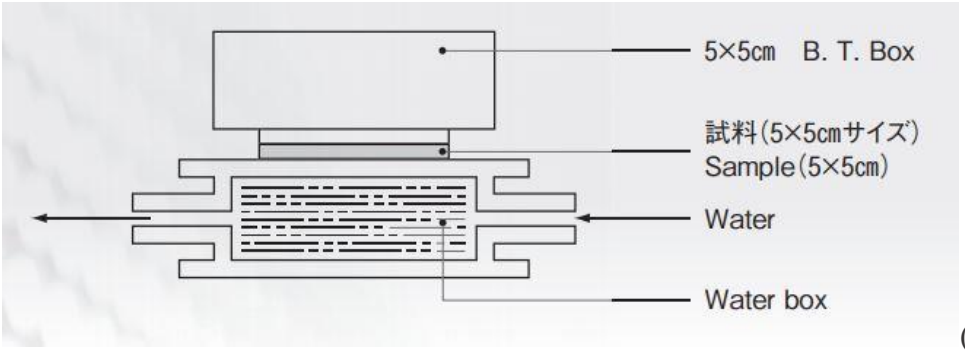

(b)

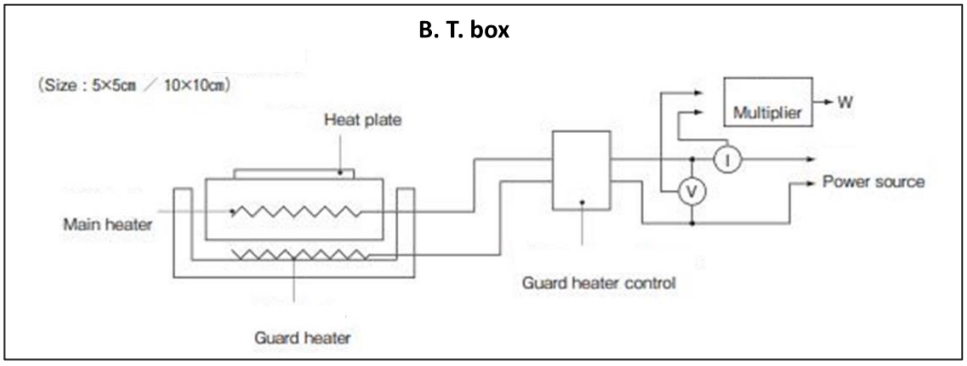

(c)

Fig. 21. (a) KES-F7 Thermal Labo ⅡB precision rapid thermal property measurement unit (b)The structure of the thermal property measurement unit. (c) The mechanism of B. T. box.

6.4.2 Results

For the thermal conductivity analysis, there is no obvious trend of the varying chemical structures such as varying silicone chain length, varying silicone concentration and block or graft structures of PUSX. The thermal conductivity is influenced mostly by the shape of the samples. We may say that both block and graft type PUSX nanofibers have much lower conductivity than films because of the pores keeping air inside. The heat insulating property is proved here. This result can be explained by the heat retaining property of nanofibers because of the high porosity.

Worth mentioning that in solid objects, heat transfer through it is via conduction. For

electrospun structures, much of the volume is made of empty spaces between fibers. Usually, the conduction along the fiber as part of the whole volume is negligible. But if the fibers get too compact, the packing density will be increased beyond an optimum standard, heat transfer via conduction through the solid fiber becomes significant and the overall insulation property will be decreased. The insulation property of electrospun nanofibers are more controllable by the packing density compared to film to meet the demands of the market. As an ideal alternative of PUSX films, PUSX nanofibers provides the heat insulating property and lightness in weight.

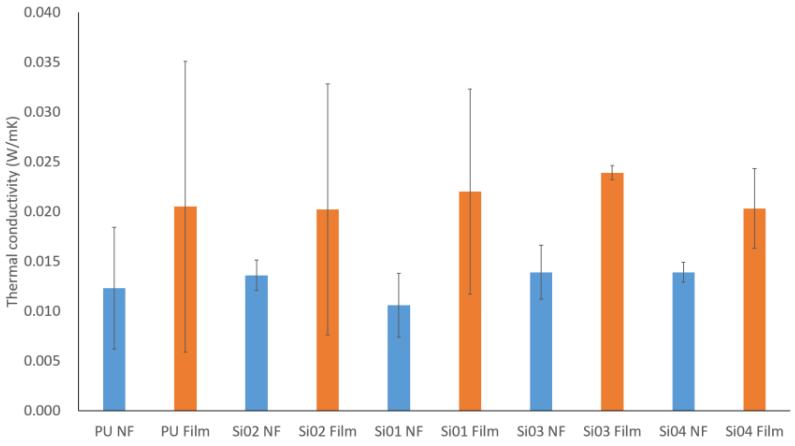

(a)

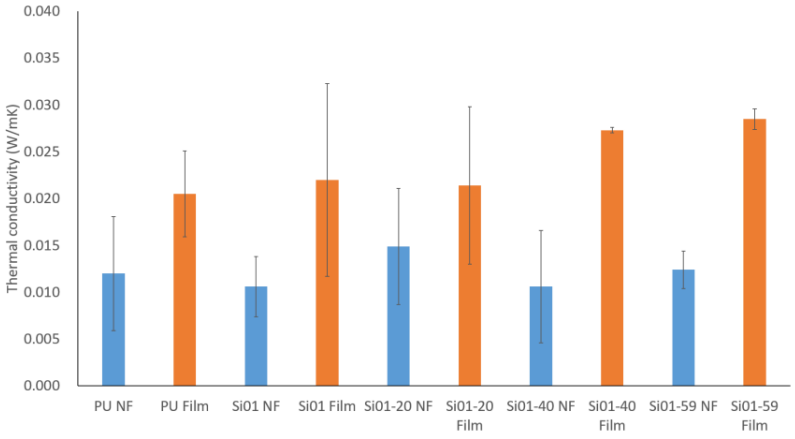

(b)

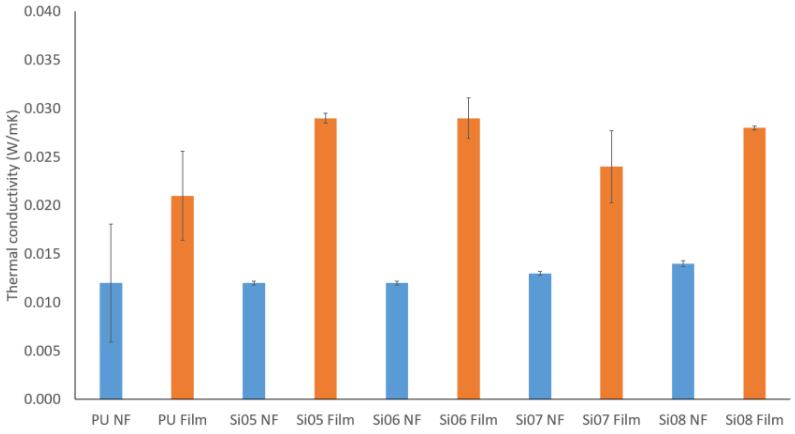

(c)

Fig. 22. Comparison of thermal conductivity (W/mK). (a) Block type PUSX nanofibers and films with various chain length, (b) Block type PUSX nanofibers and films with various silicone concentration, (c) Graft type PUSX nanofibers and films with various chain length.

6.5 Water retention and water contact angle (WCA)

Wetting ability is one of the most significant factor of evaluating nonwoven fabrics which has received tremendous interest from both fundamental and applied points of view. In recent years, there has been an increasing interest in the study of hydrophobic surfaces, due to their potential applications in, for example, self-cleaning, nanofluidics, and electrowetting. [25-28] Wettability studies usually involve the measurement of water retention value and water contact angles.

6.5.1 Experiments

Water retention tests were performed based on JIS L 1913 6.9.2. The electrospun PUSX nanofibers and films with size of 100 × 100 mm^2 were put in distilled water for a period of 15 min and then weighed. Water retention capacity was determined as the increase in the

weight of the fibers. The percentage of water absorption was calculated as following equation:

$$m = (m_2-m_1)/m_1 \times 100\%$$

where m_2 and m_1 are the weight of samples in wet and dry environment, respectively.

The water contact angle (WCA) is an easy measurement to determine the wettability of materials by a liquid. The static contact angle of pure water for the surface of PUSX samples was measured by an automated contact angle meter (DM-501Hi, Kyowa Interface Science Co., Ltd) after dripped 2 μl of purified water on the randomly surface of samples. The droplet on the samples was captured after 1000 msec through the image analyzer and the water contact angle (WCA) θ was calculated by the software through analyzing the shape of the drop.

When depositing a droplet onto the material, the water will form a drop shape. The point where the surface, the water and vapor meet, is called the three-face point and it determines the contact angle. The relationship between the contact angle, the surface free energy, the liquid surface tension and the interfacial tension between solid and liquid is defined by the Young equation:

$$\gamma S = \gamma L \cos\theta + \gamma SL,$$

where θ is contact angle, γL is the surface free energy of the solid and γSL is the interfacial tension between solid and liquid.

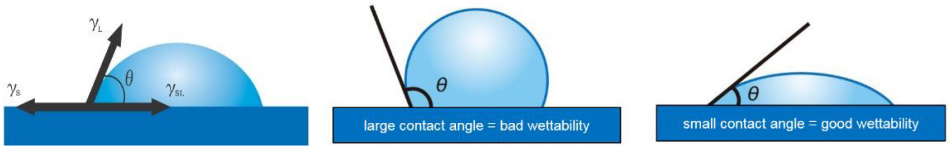

Fig. 23. The mechanism of contact angle.

Usually, when the water contact angle (CA) is less than 90^{o}, the material can be considered as hydrophilic while the material is hydrophobic. Worth mentioning that if the CA is between 150^{o} and 180^{o}, it shows the high water repellency of the material.

6.5.2 Water retention

In Table 7, there is a huge gap between pure PU and PUSX nanofibers when the PU nanofibers showed the highest water retention of 280% with statistical significance ($p < 0.05$). Block type PUSX nanofibers showed a decreasing trend in water retention with the increase of both silicone chain length and silicone concentration because of the hydrophobicity of silicone. This also means that the water repellency of PU nanofibers is able to be improved by introducing the silicone groups into the main chain. Meanwhile, compared with films, since nanofibers have high porosity to hold water, the water retentions of nanofibers are higher than films. Both PU nanofibers and films have the highest water retention. Higher hydrophobicity of silicone structure and moisture permeability were proved.

Meanwhile, for graft type PUSX nanofibers, the silicone groups on the side chain are not able to increase the hydrophobicity of the material so that the water retention did not show any difference between PU nanofibers and graft type PUSX nanofibers.

Table 7. Comparison of water retention.

Block type PUSX with different silicone chain length	PU	Si02	Si01	Si03	Si04
Nanofiber Water retention (%)	280.0 ± 40.0	27.0 ± 11.0	19.0 ± 8.1	11.0 ± 4.1	12.0 ± 2.5
Film Water retention (%)	2.3 ± 1.5	2.7 ± 1.1	1.5 ± 0.2	5.8 ± 5.0	3.7 ± 1.1
Block type PUSX with different silicone concentration	PU	Si01	Si01-20	Si01-40	Si01-59
Nanofiber Water retention (%)	280.0 ± 40.0	19.0 ± 8.1	4.7 ± 3.1	2.7 ± 0.9	6.9 ± 6.0
Film Water retention (%)	2.3 ± 1.5	1.5 ± 0.2	3.7 ± 0.7	2.7 ± 1.0	2.9 ± 2.3
Graft type PUSX	PU	Si05	Si06	Si07	Si09
Nanofiber Water retention (%)	280.0 ± 40.0	169.0 ± 23.3	196.0 ± 28.8	165.0 ± 55.0	200.0 ± 13.5
Film Water retention (%)	2.3 ± 1.5	2.3 ± 2.6	6.6 ± 7.5	6.8 ± 3.8	1.7 ± 0.9

6.5.3 Water contact angle

Fig. 24 exhibits that the water contact angles of PU are much lower than PUSX for both nanofibers and films. This phenomenon might be caused by the high hydrophobicity of silicone structure. It also proved the results of water retention when comparing PU and PUSX materials. PUSX nanofibers showed higher WCA than films because the surface of nonwoven nanofiber membrane is much rougher than films. The pores of nanofibers make the surface microstructure similar to the lotus structure of Cassie's state. (Fig. 24h)

Worth mentioning that for graft type PUSX nanofibers, the water retention appears to be high compared with block type PUSX nanofibers but the results of water contact angle are similar. This might be caused by the different surfaces of block type and graft type nanofibers. We supposed that the silicone groups distributed differently on graft type PUSX nanofibers compared with block type PUSX nanofibers.

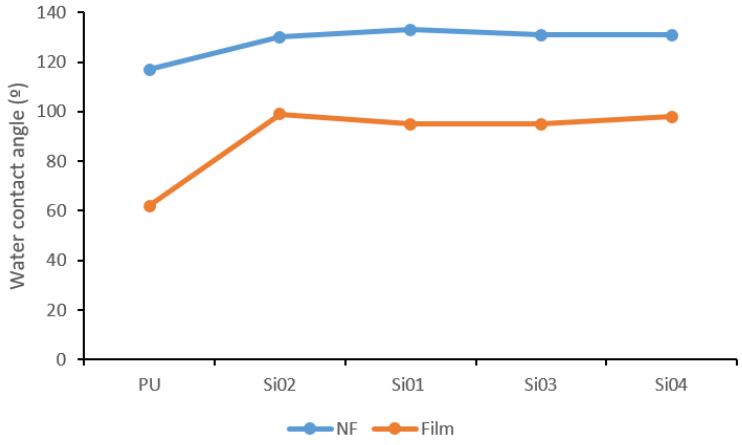
Water contact angle (º)
140
120
100
80
60
40
20
0
PU
Si02
Si01
Si03
Si04
NF
Film

(a)

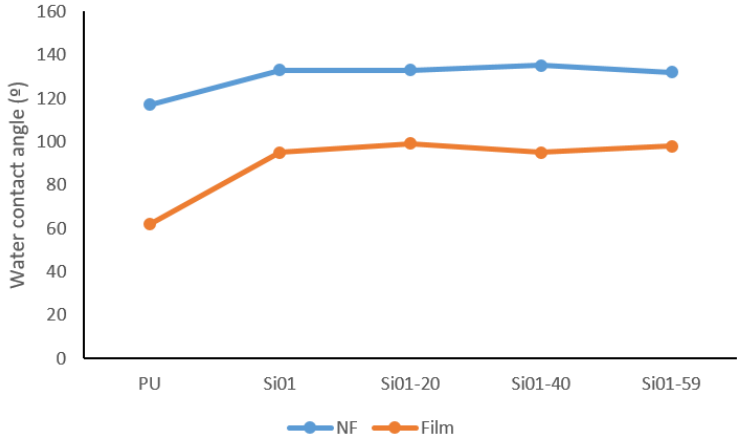
Water contact angle (º)
160
140
120
100
80
60
40
20
0
PU
Si01
Si01-20
Si01-40
Si01-59
NF
Film

(b)

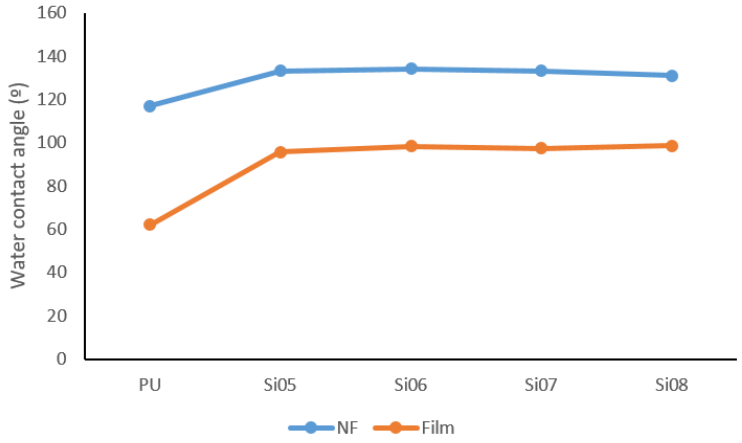
Water contact angle (º)
160
140
120
100
80
60
40
20
0
PU
Si05
Si06
Si07
Si08
NF
Film

(c)

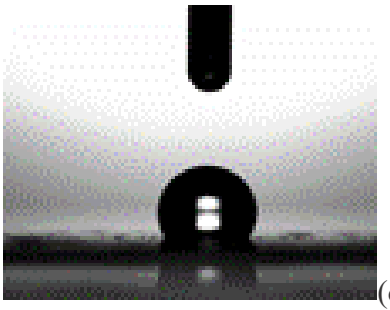
(d)

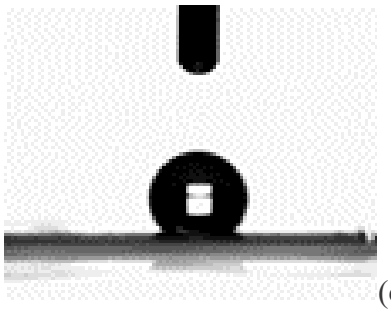
(e)

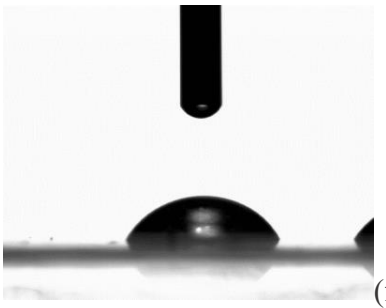
(f)

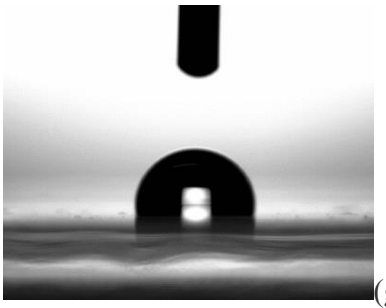
(g)

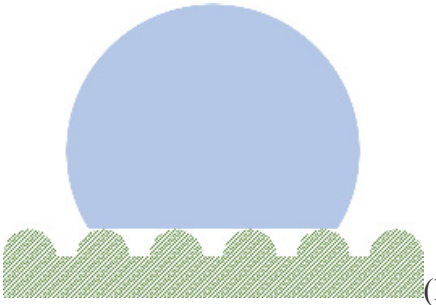
(h)

Fig. 24. Comparison of water contact angle (deg). (a) Block type PUSX nanofibers and films with various chain length, (b) Block type PUSX nanofibers and films with various silicone concentration. WCA images of (d) PU nanofibers, (e) PUSX Si08 nanofibers, (f) PU films, (g) PUSX Si08 films and (h) Lotus microstructure (Cassie's state)

6.6 Conclusion

In the present chapter, we investigated the physical properties and biocompatible properties of PUSX nanofibers and compared with films. As a conclusion of all the physical

properties analysis, mechanical properties, water retention and water contact angle (WCA) can be controlled and improved by adjusting the structure. Unfortunately, the graft type PUSX did not show obvious changes in mechanical strength because the side chains of silicone could not make as much influence as the main chain of PU does. But we may say that the graft type PUSX nanofibers can be the most similar alternative of PU nanofibers in mechanical properties but with better water repellency. Higher hydrophobicity and lower thermal conductivity were also found in PUSX nanofibers thanks to the unique advantages of nanofibers compared with films.

We can expect this material to be applied in various fields. For instance, by controlling the silicone chain length and concentration of block type PUSX nanofibers, we may apply it in medical field such as bandage or scaffold, apparel field such as outdoor goods and sportswear, also we can use it as air or water filters.

6.7 References

[1] Thandavamoorthy Subbiah, et al. Electrospinning of nanofibers, Journal of Applied polymer science, Volume 96, Issue 2, pp 557-569, 2005,

[2] Viness Pillay, et al. A Review of the Effect of Processing Variables on the Fabrication of Electrospun Nanofibers for Drug Delivery Applications, Journal of Nanomaterials, Volume 2013, 2013.

[3] X. Liu, et al. Polymeric scaffolds for bone tissue engineering, Annals of Biomedical Engineering, Volume 32, No. 3, pp 477-486, 2004.

[4] Z.G.Chen, et al. Electrospun collagen–chitosan nanofiber: A biomimetic extracellular matrix for endothelial cell and smooth muscle cell, Acta Biomaterialia, Volume 6, Issue 2,

pp 372-382, 2010.

[5] Wenying Liu, et al. Electrospun Nanofibers for Regenerative Medicine, Advanced Healthcare Materials, Volume1, Issue1, pp 10-25, 2012.

[6] Esra KiliçArzu YakarNursel Pekel Bayramgil. Preparation of electrospun polyurethane nanofiber mats for the release of doxorubicine, Journal of Materials Science: Materials in Medicine, 2018.

[7] Lionelli GT, et al. Wound dressing, Surg Clin North Am. 2003; 83: pp 617-638, 2003.

[8] Thomas S. Wound management and dressings, Pharm P. 1990;1, pp 37-57, 1990.

[9] Bhardwaj N, et al. Electrospinning: a fascinating fiber fabrication technique, Biotechnol Adv. 2010;28: pp 325-347, 2010.

[10] S.R. Bhattarai, et al. Novel biodegradable electrospun membrane: scaffold for tissue engineering, Biomaterials, Volume 25, pp 2595-2602, 2004.

[11] A. Suthar, et al. Nanofibres in filter media, Chem Eng, 726, pp 26-28, 2001.

[12] A. Chatterjee, et al. Carbon nanotubes and nanofibre: an overview, Fiber Polym, 3 (4), pp 134-139, 2002.

[13] S. Sundararajan, et al. Mechanical property measurements of nanoscale structures using an atomic force microscope, Ultramicroscopy, 91 (1–4), pp 111-118, 2002.

[14] E.P.S.Tan, et al. Mechanical characterization of nanofibers – A review. Composites Science and Technology, Volume 66, Issue 9, pp1102-1111, 2006.

[15] R.W. Zimmerman. Compressibility of Sandstones. Elsevier Science Publisher Co., New York, 1991.

[16] D.B. Ingham, et al. Emerging Technologies and Techniques in Porous Media, Kluwer Academic Publishers, London, 2003.

[17] A. Sayari, et al. Nanoporous Materials IV, Elsevier Science Publisher Co., New York, 2005.

[18] D.B. Ingham, I. Pop. Transport Phenomena in Porous Media III. Elsevier Science Publisher Co., Oxford, UK, 2005.

[19] N. Pan, W. Zhong. Fluid Transport Phenomena in Fibrous Materials. Woodhead Publishing Ltd., Cambridge, UK, 2006.

[20] J. Kuhn, et al. Thermal transport in polystyrene and polyurethane foam insulations. Int. J. Heat Mass Transfer, 35 (7), pp. 1795-1801, 1992.

[21] G.O. Hanser. Polyurethane Handbook: Chemistry, Raw Materials, Processing, Application, Properties. Hanser Publishers, New York, 1994.

[22] J.W. Wu, et al. Thermal conductivity of polyurethane foam, Int. J. Heat Mass Transfer, 42, pp 2211-2217, 1999.

[23] W.H. Tao, et al. Measurement and prediction of thermal conductivity of open cell rigid polyurethane foam. J. Cell. Plast., 37, pp 310-331, 2001.

[24] C.J. Tseng, et al, Thermal conductivity of polyurethane foams from room temperature to 20 K, Cryogenics 37 (6), pp 305-312, 1997.

[25] M. Rauscher, S. Dietrich, Annu. Rev. Mater. Sci. 38, 143, 2008.

[26] K. Fei, C.P. Chiu, C.W. Hong, Microfluid. Nanofluid. 4, 321, 2008.

[27] Z. Keshavarz-Motamed, L. Kadem, A. Dolatabadi, Microfluid. Nanofluid. 8, 47, 2010.

[28] Y.S. Nanayakkara, S. Perera, S. Bindiganavale, E. Wanigasekara, H. Moon, D.W. Armstrong,Anal. Chem. 82, 3146, 2010.

Chapter 7

In vitro biocompatible evaluation

7 In vitro biocompatible evaluation

7.1 Introduction

Since the aim of this research is figure out the potential of PUSX nanofibers as an alternative of PU nanofibers and PU films in biomedical applications. Our discussion is mainly focused on nanofibrous scaffold for tissue engineering and wound dressing material. In order to reveal the potential in cell adhesion and proliferation, NIH3T3 mouse embryonic fibroblasts cells were cultures on all the samples following by LDH activity. The toxicity of PUSX nanofibers and films was evaluated by using direct contact based on ISO 10993-5. We supposed that PUSX nanofibers could become an ideal alternative of PU membranes in biomedical fields by investigating the physical properties in Chapter 6 and biocompatibility in this chapter.

7.2 Cell culture studies

7.2.1 Experiments

Before applying samples to in vitro cell culture, it is essential to remove the DMF/MEK mixed solvents because of the possible cytotoxicity. All the samples were washed with distilled water for 48h and dried in oven at 80℃ overnight. Then, the nanofibers and films were cut into round shape with a diameter of 10 mm, preparing 3 replicates per sample. The sterilization was performed by deeply soaking the samples in 70% ethanol aqueous solution in a multi-well TCPS dish for 1h followed by rinsing 3 times in PBS to remove all traces of ethanol.

NIH3T3 mouse embryonic fibroblasts were used to measure the cell adhesion and

proliferation. As one of the most commonly utilized cell lines, the NIH3T3 cell line has been incorporated in studies for a range of mechanistic and cell based assays, including protein functional analysis. The morphology of the cells are adherent, fibroblastic and are considered to be among the relatively easy to grow cell lines. For the cell adhesion test, 50,000 cells (in 1 ml of medium) were poured in the sample well. After 3 h, the cells were harvested in 1 ml of 0.5% Triton X-100/PBS solution and evaluated by LDH assay to give the cell adhesion evaluation.

The cell proliferation test was a quantitative investigation of the capacity for cell to grow on the electrospun nanofibers and films. The experiment lasted for a total of 7 days and the results of the 1^{st}, 3^{rd}, 5^{th} and 7^{th} day were compared.

The LDH activity was immediately measured by ultraviolet absorption at wavelength 340 nm using Thermo Scientific Multiskan FC microplate photometer (Thermo Fisher Scientific Inc.) with recorder. The enzyme activity of LDH can measure from chemical reaction of LDH when it is released into the cells medium from the damaged or dead cells due to cell membrane damage. LDH converts lactate using NAD as a coenzyme and produces pyruvic acid and NADH. The number of cells was calculated from calibration curve obtained by the relation between the known number of cells and absorbance value at 340 nm of NADH in the assay supernatant.

The shape of cells was observed by SEM to investigate qualitatively the cells reaction in contact with the electrospun nanofibers. After each incubation period, the sample was fixed with paraformaldehyde (PFA) as cross-linking fixation agent to stop the proliferation of cells and preserve their shape. Samples were further dehydrated by using each ethanol gradient solution of 50, 70, 95, and 99.5% for 30 min by continuous process. Then the

sample was coated with platinum for SEM analysis.

Significance in vitro biocompatibility was statistically analyzed by one-way analysis of variance (ANOVA) using R free software. Statistical significance was set at $p < 0.05$ to identify which group were significantly different from other groups.

7.2.2 Results

To investigate the in vitro biocompatibility of blend nanofibers, NIH3T3 cells were cultivated on PUSX nanofibers and films of different structures. Cell attachment results were obtained and calculated after 3h and showed in Fig. 25. As the result, the number of adhered cells on block type PUSX nanofibers became higher with the increase of silicone chain length. The reason of the increase of fibroblast cells might be due to NIH3T3 cells being easily grown on the surface which has higher water repellency and hydrophobic surface characteristics. As we discussed in chapter 6, a higher water repellency is found with the increase of silicone chain length in block type PUSX nanofibers.

The cell attachment results of PUSX films were not shown due to the very low number after 3h. Cells take shorter time to adhere on nanofibers than on films because of the porosity of electrospun nanofibers. For cell attachment, we may get the conclusion that PUSX nanofibers are more suitable than films.

Table 8 represents the SEM images of NIH3T3 fibroblast cells cultured for 3 days on different PUSX nanofibers and films with different structures. It can be seen that after 3 days culture, there are more cells on films than on nanofibers, but the entanglement of cells is totally different. The cells attached in the pores of nanofibrous membranes with rough surface are much easier for tissue engineering as a scaffold. The stability is much higher

than the cells attached on the surface of films. The reason might be that nanofibers with a fiber diameter of 400–700 nm mimic extracellular matrix (ECM) as well as the pores helping the cells to stay stable in the membranes. This work suggested that PUSX nanofiber has an important advantage of being able to physically biomimic the natural ECM for tissue engineering applications and cell ingrowth and cell encapsulation in nanofibrous scaffolds are equally important. The architecture of a scaffold and the material used to play an important role in modulating tissue growth and response behavior of the cells which have been cultured onto the scaffold. In this regard, the scaffold should not only work as a substrate for cell attachment, growth and proliferation, but also facilitate cell migration, ingrowth and assembly into a stereo-structure. From the SEM morphologies, we are able to see that the cells did attach on PUSX nanofibers better than on films because of the porosity makes nanofibers more stereo than films. Besides that, since the mechanical property, the topographical layout, and the surface chemistry in the nonwoven mat may have a direct effect on cellular proliferation and migration.[1] The electrospun mat may provide mechanically stable scaffolding, in which cells can proliferate. Then, the cells synthesize their own extracellular matrix to form a functional tissue while the electrospun mat degrades away.

Fig. 26 shows the cell proliferation results after 1 day, 3 days, 5 days and 7 days respectively. All 12 kinds of PUSX nanofibers are proved to be appropriate for cell proliferation with the maximum cell number around more than10000 on the 5th day. PUSX nanofibers can be applied in biomedical filed as a better alternative of PU nanofibers with controllable physical properties because of the similar results of cell proliferation test. As a result, we are able to prepare biomedical materials of desired physical properties by

changing the structure without losing the same level of biocompatibility.

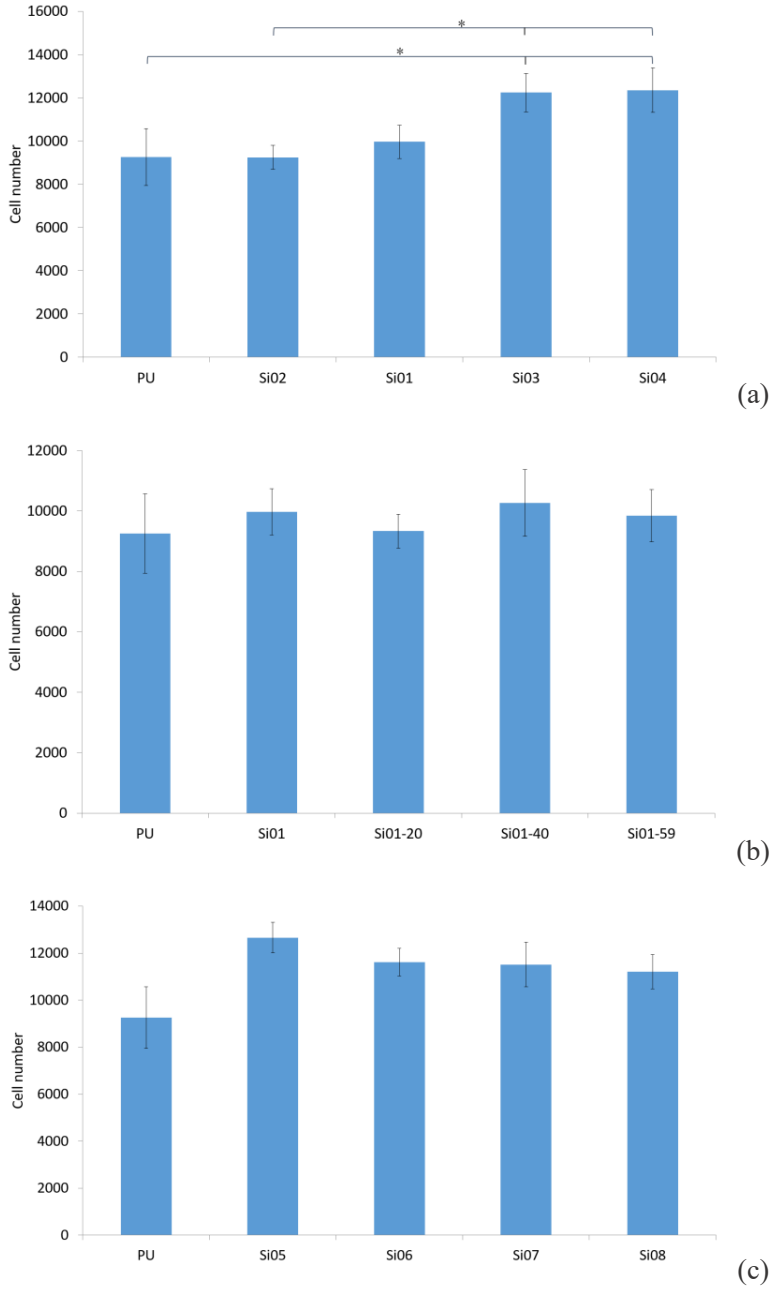

Fig. 25. The attachment of NIH3T3 cells, (a) Block type PUSX nanofibers with various chain length, (b) Block type PUSX nanofibers with various silicone concentration, (c) Graft type PUSX nanofibers after cells attached for 3 hours. "*" is statistically significant ($p < 0.05$) between each 2 samples.

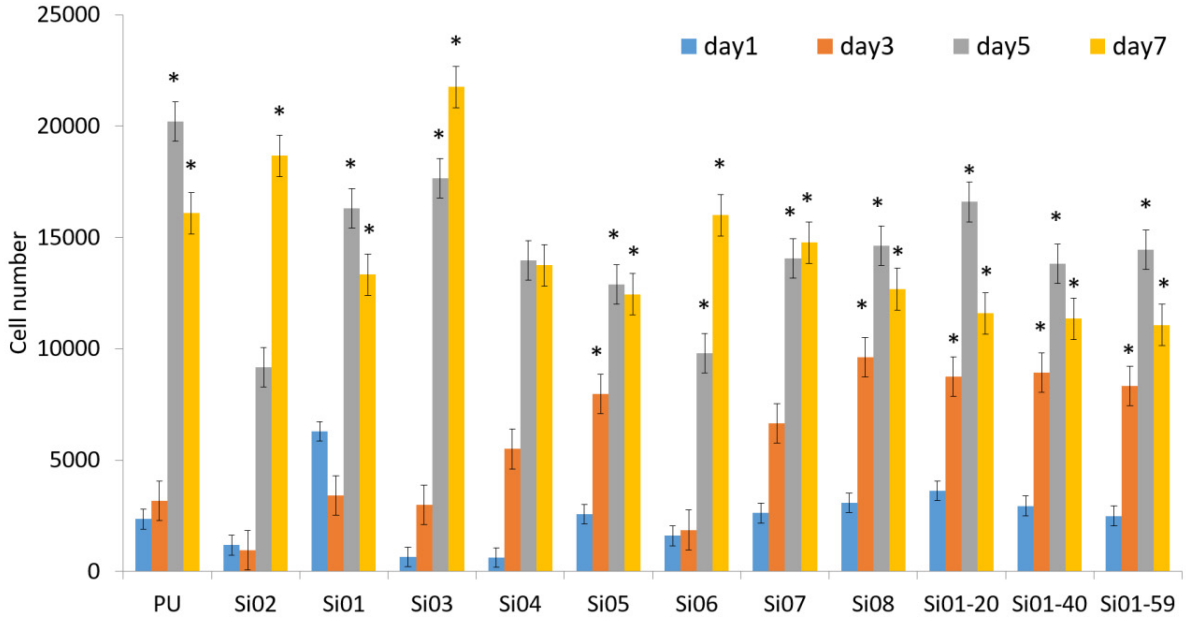

Fig. 26. The proliferation of NIH3T3 cells on Block type PUSX nanofibers with various chain length, Block type PUSX nanofibers with various silicone concentration and Graft type PUSX nanofibers after cells cultured for 1, 3, 5, and 7 days, respectively.

Table 8. SEM images of NIH3T3 cells where cultured for 3 days on each sample.

	PU	Si02	Si01	Si03	Si04
NF (×1000)	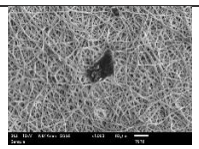	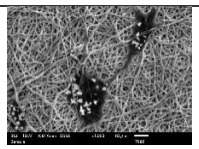	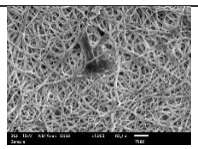	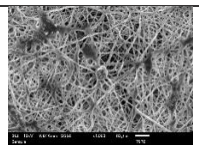	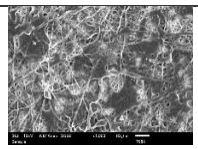
FILM (×500)	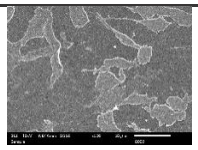	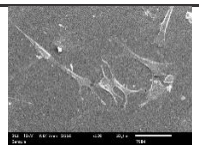	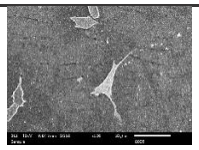	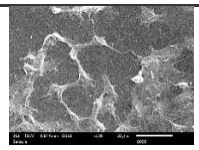	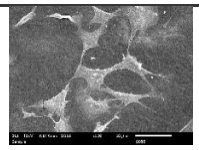
	PU	Si01	Si01-20	Si01-40	Si01-59
NF (×1000)	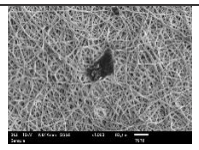	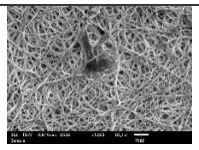	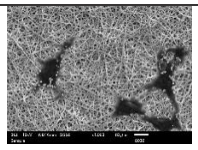	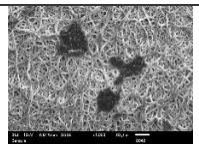	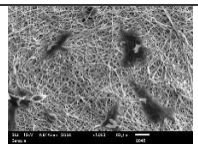
FILM (×500)	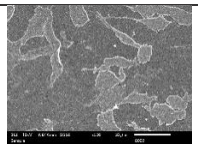	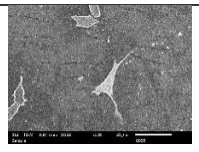	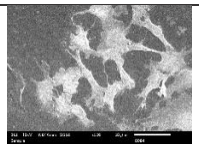	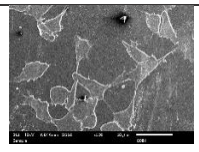	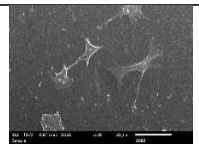
	PU	Si05	Si06	Si07	Si08
NF (×1000)	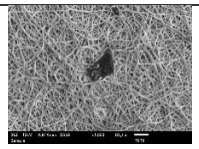	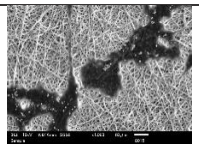	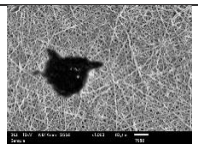	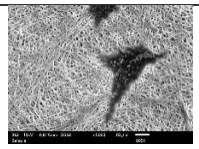	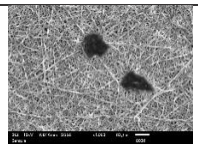
FILM (×500)	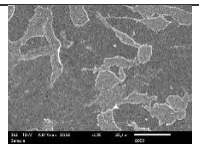	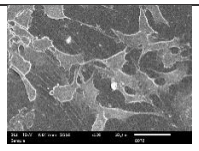	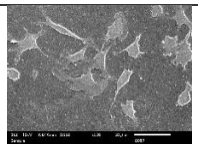	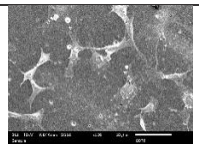	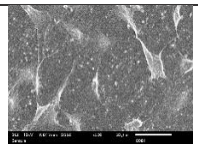

7.3 Toxicity evaluation

7.3.1 Experiments

The toxicity of PUSX nanofibers and films was evaluated by using direct contact based on ISO 10993-5. Briefly, cells were seeded evenly over the surface of each plate and incubated at 37 ◦C until the cells covered the whole surface. The samples were then placed

on the cells layer in the center of the plates and the culture medium was replaced. In order to determine the toxicity in accordance with grade 0 (nontoxic) to grade 4 (severe toxic) evaluation, trypan blue was added after 24 h in each plate and observed by morphological changes. This is the most obvious and direct way to reflect the impact of testing the materials on the cell.[2]

7.3.2 Results

The results as displayed in Table 9 showed that both the PUSX films and nanofibers caused less toxicity in contact with cells. The cells are able to keep the spreading shape and discrete intracytoplasmic granules with no cell lysis, which can be considered as survival compared with positive control (cells became round and layers were completely destroyed). The morphological grade of cytotoxicity is supposed to be 0.

There is no obvious difference between PUSX and PU material because of the biocompatibility of silicone. To the best of our knowledge, silicone has been extensively used in medical areas, in several products such as breast implants, contact lenses, lubricants, sealers, artificial cardiac tubes and valves, urethral and venous catheters, membranes for blood oxygenation, dialysis tubes, orthopedic applications and facial reconstructions because of the high biocompatibility.[3, 4] The existence of silicone group does not change the biocompatibility of the material. From these results, we may suppose that PUSX materials have suitable biocompatibility for use as biomedical materials, such as waterproof bandage or scaffold for tissue engineering.

Table 9. The toxicity evaluation of PU and PUSX nanofibers and films.

	PU	Si01	Si02	Si03	Si04
Nanofiber		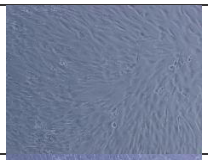	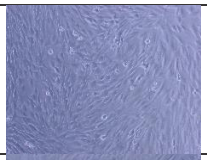	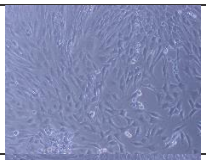	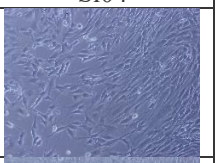
Film			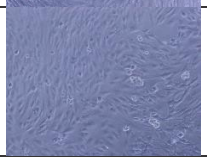	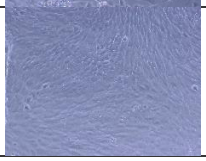	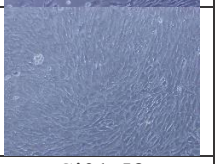
	PU	Si01	Si01-20	Si01-40	Si01-59
Nanofiber	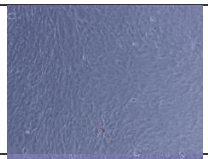	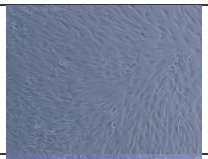	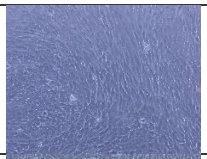	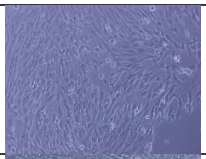	
Film	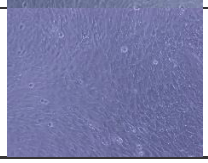		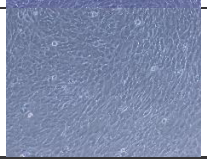	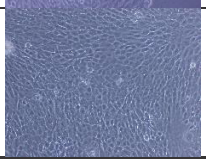	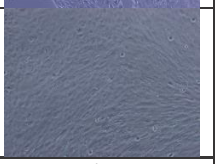
	PU	Si05	Si06	Si07	Si08
Nanofiber		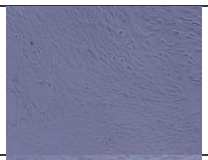			
Film		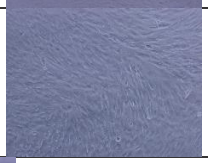			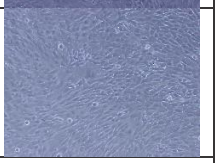
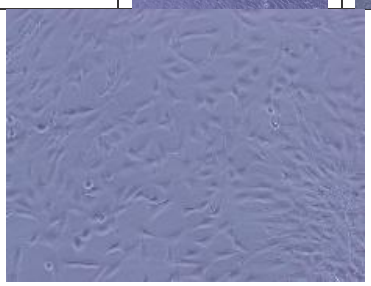 (Negative control)			 (Positive control)		

7.4 Conclusion

In vitro biocompatible evaluation shows that the cell proliferation can be performed on both PUSX nanofibers and films. But for cell attachment, cells are not able to attach on PUSX films in a short time nor entangle in the material, PUSX nanofibers were proved to be more appropriate for cell culture study. For the regeneration of tissue engineering, the proved biocompatibility of PUSX fibrous scaffolds are generally preferred because of the unique nature and ability to provide the target cells/tissues with a native environment by mimicking the extracellular matrix. For wound dressing, since PUSX nanofiber is proved to be more hydrophobic than PU nanofibers, providing a difficult environment for the bacterial adhesion and phagocytic ingestion. Electrospun PUSX nanofibers with highly controllable physical properties have been successfully proved to be an ideal alternative of PU membranes in biomedical fields.

7.5 References

[1] Surawut Chuangchote, Pitt Supaphol. J. of Nanosci. and Nonotech. 6: pp 125-129, 2006.

[2] ISO10993-5, Biological evaluation of medical devices, Part 5: Tests for in vitro cytotoxicity, 2009.

[3] Quatela VC, et al. Synthetic facial implants. Facial Plast Surg Clin North Am, pp 1-10, 2008.

[4] Chin T, et al. Experimental analysis of silicone leakage. J Nippon Med Sch, 76, pp 109-112, 2009.

Chapter 8

Conclusions and outlook

8 Conclusions and outlook

8.1 Conclusions

In the present study, we successfully prepared 12 kinds of PUSX nanofibers under the optimized conditions and investigated the effects of solvents and solution concentrations on the electrospinnability of PUSX solutions along with the morphological appearance of the as-spun nanofibers and chemical structures were all characterized. This is the first time we suggest a way of preparing PUSX nanofibers during past decades instead of making silicone and PU into composite and then preparing into nanofibers or films. Various surface morphologies, including beads, bead-on-string structure, as well as fibers with different diameters and shapes, were formed. In addition, a study of the reproducibility and feasibility of the electrospinning parameters was performed on a pilot scale electrospinning set-up. On both lab scale device and pilot scale set-up PUSX solutions could be successfully electrospun. Hence, the present work has demonstrated the great potential of the electrospinning process for the production of PUSX nanofibrous sheets from solutions. We believe that PUSX nanofibers might become a new alternative to PU nanofibers or composites in many potential fields.

As a conclusion of all the physical properties analysis, mechanical properties, water retention and water contact angle (WCA) can be controlled and improved by adjusting the structure. Unfortunately, the graft type PUSX did not show obvious changes because the side chains of silicone could not make as much influence as the main chain of PU does. Higher hydrophobicity and lower thermal conductivity were also found in PUSX nanofibers. We can expect this material to be applied in various fields. For instance, by controlling the silicone chain length and concentration of block type PUSX nanofibers, we

may apply it in medical field such as bandage or scaffold, apparel field such as outdoor goods and sportswear, also we can use it as air or water filters.

In vitro biocompatible evaluation shows that the cell proliferation can be performed on both PUSX nanofibers and films. But for cell attachment, cells are not able to attach on PUSX films in a short time nor entangle in the material, PUSX nanofibers were proved to be more appropriate for cell culture study. Electrospun PUSX nanofibers have been successfully proved to be an ideal material in biomedical applications such as wound dressing and tissue engineering thanks to the excellent physical properties and biocompatibility.

8.2 Outlook (PUSX/TiO_2 blend nanofibers)

As for future research, it is essential to evaluate the antibacterial effect by electrospinning the PUSX nanofibers and antibacterial agents together and perform the test against Staphylococcus aureus and Escherichia coli. The prepared antibacterial agent/PUSX nanofibrous matrix could be properly employed as recommended candidate for many biological applications such as internal aid for water and air filters membranes and for prolonged antimicrobial wound dressing agents.

Antimicrobial nanocomposites based on titania (TiO_2) have been actively investigated in recent years. Titania has substantial advantages over both chemical (NO, H_2O_2, small organic molecules) and metal (typically Ag)-based systems.[1, 2] First, titania nanoparticles have a broad spectrum of activity against microorganisms, including Gram-negative and positive-bacteria and fungi, which is of particular importance for multiple drug resistant strains.[1, 2] Second, and more importantly, titania-polymer nanocomposites are intrinsically

environmentally friendly and exert a non-contact biocidal action. Therefore, PUSX/TiO2 blend nanofibers were recently prepared by electrospinning the PUSX Si01/ TiO_2 blend solution under varying ratio. The antibacterial evaluation against Staphylococcus aureus and Escherichia coli.is expected in future experiments. This material is supposed to be appropriate for biomedical applications and attract more and more interest as the alternative of PU nanofibers and films.

8.3 Reference

[1] Wiener, J. et al. Multiple antibiotic–resistant Klebsiella and Escherichia coli in nursing homes. J. Am. Med. Assoc. 281, 517–523 (1999).

[2] Josset, S., Keller, N., Lett, M. C., Ledoux, M. J. & Keller, V. Numeration methods for targeting photoactive materials in the UV-A photocatalytic removal of microorganisms. Chem. Soc. Rev. 37, 744–755 (2008).

Publications

The dissertation is based on the following published papers.

Journal of articles

• Chuan Yin, Rino Okamoto, Mikihisa Kondo, Toshihisa Tanaka*, Hatsuhiko Hattori, Masaki Tanaka, Hiromasa Sato, Shota Iino, Yoshitaka Koshiro. Electrospinning of block and graft type silicone modified polyurethane nanofibers. Nanomaterials, 2019, 9, 34, doi: 10.3390/nano9010034.

• Chuan Yin, Sélène Rozet, Rino Okamoto, Mikihisa Kondo, Yasushi Tamada, Toshihisa Tanaka*, Hatsuhiko Hattori, Masaki Tanaka, Hiromasa Sato, Shota Iino. Physical properties and in vitro biocompatible evaluation of silicone modified polyurethane nanofibers and films. Nanomaterials. SI: Electrospun Nanofibers for Biomedical Applications, 2019, 9, 367, doi: 10.3390/nano9030367.

Conferences

A part of the dissertation was presented in conferences as the following.

Oral presentations

• The 10th International Conference of Modification, Degradation and Stabilization of Polymers, Sep 2nd~6th, 2018, Tokyo, Japan (OC-1-09). Fabrication and physical analysis of silicone modified polyurethane nanofibers.

Poster presentations

• Workshop of Advanced Composites (WAC) 2017, Nov 10th ~12th, 2017, Ueda, Japan. (PP-03). Preparation and characterization of silicone modified polyurethane nanofibers.

• The 3rd International Symposium on Nanoparticles/Nanomaterials and Applications, Jan 22nd~25th, 2018, Costa de Caparica, Portugal (P-20). Characterization and preparation of silicone modified polyurethane nanofibers.

• 第 67 回高分子学会年次大会, 2018 年 5 月 23 日 ~ 25 日, 名古屋(3Pd094). 異なる分子構造を有するシリコーン変性ポリウレタンナノファイバーの物性比較

Comparison of physical properties for silicone modified polyurethane nanofibers with different molecular structures.

• Textile Summit 2018, Sep 20th~22nd, 2018, Ueda, Japan. Preparation and Physical Properties of Silicone Modified Polyurethane Nanofibers with Different Molecular Structures.

Acknowledgments

I would like to express my deepest gratitude to Professor Toshihisa Tanaka for the guidance and insight in supervising the research, his invaluable help and kindness. The supports and encouragements enable me to accomplish this dissertation.

Special thanks to Professor Masayuki Takatera, Professor Qingqing Ni and Professor Yasushi Tamada, Professor Tadahisa Iwata and Professor Xiangqiang Pan for their insightful comments and advices.

I sincerely appreciate a Grant-in-Aid for the Shinshu University Advanced Leading Graduate Program provided by the Ministry of Education, Culture, Sports, Science and Technology of Japan for the financial support, overseas education opportunities, job hunting and mentoring support. Sincere thanks to all the professors and secretary staffs in this program for their generous support, frank advices and warm encouragement in every aspect during the past 5 years.

I would like to thank Shin-Etsu Chemical Co., Ltd and Dainichiseika Color & Chemicals Mfg. Co., Ltd. for kindly supplying the materials and insightful comments in this research.

I would like to express my gratitude to the technicians and students who involved in this research for their patience and supports. Special thanks to Ms. Sélène Rozet for her generous support in experiments, warm encouragement in every aspect in my life and precious friendship. Also, this dissertation may not be fulfilled without the preceding study of Ms. Rino Okamoto, Mr. Mikihisa Kondo and Ms. Hiroko Ide.

Finally, I would like to appreciate the members of Tanaka Laboratory and Leading Graduate Program for their great support and warm friendship.